CZECH UNIVERSITY OF LIFE SCIENCES PRAGUE

Faculty of Agrobiology, Food, and Natural Resources

Department of Water Resources

Assessing the Function of Controlled Drainage Using Satellite Data

DIPLOMA THESIS

Teshome Manyazewal

Natural Resources and Environment

Supervisor: Ing. Kamila Báťková, MSc., PhD.

Co. Supervisor: Ing. Václav David, PhD.

Declaration

I hereby declare that I have completed this thesis titled "**Assessing the function of controlled drainage using satellite data"** by myself. And all the sources I cited in the thesis are listed in the references. As the master's thesis author, I declare that the thesis does not break any copyrights.

In Prague, April 14, 2022 .....

Teshome Manyazewal

Acknowledgment

I would like to thank almighty GOD for making all this possible. I would like to express my gratitude to my supervisor Dr. Kamila Báťková (MSc., PhD) for all her support and guidance she gave me throughout the writing process. I would like to acknowledge Dr. David Václav (PhD) for the technical advice he gave me. I would like to extend my heartfelt gratitude to all professors and members of the department for supporting me through my study time.

I am grateful to the Czech Government for supporting my master's studies and for allowing me the opportunity to pursue my academic interests and goals.

Assessing the Function of Controlled Drainage Using Satellite Data

Abstract

The amount of available water to plants is a crucial parameter in determining the yields of crops grown on agricultural land. The controlled drainage systems providing subsurface irrigation can reduce the water shortage part of the vegetation season. The conversion of the existing drainage systems in which the water level in the system can be controlled is now being researched in the Czech Republic. One of the pilot localities is in Strašov, Pardubice Region. The thesis is focused on the application of the remote sensing method for evaluation of the condition of the grown crop by comparing the normalized difference vegetation indexes (NDVI) for areas affected and unaffected by the controlled drainage. The functionality of the controlled drainage system was evaluated based on the assumption that plants' response to solar radiation reflects their water stress status. Plants highly absorb red and reflect near-infrared (NIR) bands when they are in good status. The satellite imageries were downloaded from the Land Viewer, Earth observing system (EOS). In each part of the area (affected/unaffected by controlled drainage), 10 sampling polygons were defined and the NDVI values were compared for the vegetation season from April to October 2020. The vegetation season was selected to reduce the impact of soil reflectance. Suitable dates for which the NDVI values could be compared were selected and NDVI data for these dates were then statistically evaluated by analysis of variance. For the periods when the precipitation did not meet the plants' requirements, the plants grown on the area affected by controlled drainage showed significantly higher NDVI values than plant grown on the unaffected area. The NDVI differences between the areas diminished in the period with sufficient precipitation. Later during the season when the regulation was set out of operation, the NDVI values of the two areas were similar and did not significantly differ from each other. The results support the conclusion that the NDVI analysis from the satellite data can provide information assessing the function of the controlled drainage system in the agricultural field. To prove the technique further, data for more vegetation seasons for more than one experimental sites needs to be evaluated.

Keywords: Satellite imagery, Vegetation index, Remote sensing, Normalized difference vegetation index, Drainage, Controlled drainage system

Table of Contents

1 Introduction

1.1 Background of the study

Since we are living in the twenty-first century it is very important to use modest technology in hand on every activity we conduct. One of the technologies that the modern age gave to us is the capability to assess an interest area without physical contact with the object. This capability can be realized through the remote sensing method.

> "Remote sensing is the science (and to some extent, art) of acquiring information about the Earth's surface without actually being in contact with it. This is done by sensing and recording reflected or emitted energy and processing, analysing, and applying that information." (Campbell, 1987)

The above definition is very broad. Because it is defining the term as a method of gathering information about the earth's surface. However, the definition of remote sensing in the current state of art extends to the process of acquiring data about any object without physically being there. This is true regardless of whether the onlooker is nearby the object or far away. It is additionally necessitated that such detecting might be accomplished without any issue in the interceding space between an object and the onlooker. Subsequently, the data about the item, region, or any marvel should be accessible in a structure that can be dazzled on a transporter vacuum. The data transporter, or correspondence connect, is electromagnetic energy. Remote sensing information essentially comprises frequency force data procured by gathering the electromagnetic radiation leaving the item at a frequency and estimating its power (Reddy, 2008).

But remote sensing is a very wide and detailed science. It can be active or passive, it can be satellite based or air born based, it can be high resolution or low resolution, it can be panchromatic or multispectral, and or it can be hyperspectral. All these types of remote sensing have their application area they are best on. This is due to the very fast and applied technological development through time.

Remote sensing innovation has been created from balloon photography to aerial photography to multi-spectral satellite imaging. Radiation interaction characteristics of the earth's surface and atmosphere in different regions of the electromagnetic spectrum are very useful for identifying and

characterizing the earth's surface and atmospheric features(Aggarwal, 2005). Satellites play an enormous role in the advancement of numerous innovations like world planning, Global Positioning System (GPS), City planning, and so forth. Remote Sensing is one of the numerous developments that were conceivable, because of the satellites wandering around the earth (Yadav et al., 2013). RS is being used in various fields such as used are forestry, weather, agriculture, changes detection, biodiversity, and many more.

To be more specific in the application area and subject matter of the study. It is good to discuss the application of remote sensing for monitoring vegetation and/or analysing other factors which are related to situation of vegetation. Concerning this, it is very clear that remote sensing is a viable methodology for following phenological changes, for example, leaf green-up and fall shading from the local to the worldwide scale (Motohka et al., 2010).

(Roberts, 1984) mentioned that the light interception level of plants elaborates the condition of plants. There are three basic approaches for estimating vegetation fraction from satellite data: spectral mixture analysis, neural networks, and vegetation indexes (Gitelson et al., 2002).

Spectral mixture analysis with the utilization of reference end-individuals is utilized to show reflectance information as combinations of green vegetation, non-photosynthetic vegetation, soils, and shade (Roberts, 1984). It is a compelling method to screen vegetation cover. Direct ghostly blend displaying joined with the head part investigation has permitted the appraisal of important farming and agronomic data in a characteristic scene utilizing 10 - 20 otherworldly channels (Hamed, 2005). This strategy requires auxiliary ground estimations of appropriate biophysical factors to decide the experimental connection between those factors and unmixing parts for each unique arrangement of hyperspectral information.

Rondeaux et al. (1996) effectively utilized neural networks to appraise shade hole division and indicated that it tends to be precisely assessed from Near Infrared (NIR) and Red reflectance with the solitary subordinate data being the vegetation type and soil line attributes. This 'discovery' procedure, which is reliant on the dataset utilized in the preparation cycle, is performed in a way that is better than the best vegetation record. The researchers utilized a reproduction model to give a huge dataset covering the conceivable scope of factors. The primary constraint of this methodology results from the approximations and suppositions made in the displaying of the radiative exchange, and in the dissemination of the information factors of the model. However, the

vegetation division got from the combination demonstrated just as from neural organizations is not a clear assessment of the vegetation sum and it requires cautious examination (García-haro et al., 2007).

Vegetation indices are widely used indicators of temporal and spatial variations in vegetation structure and biophysical parameters. This method has just been demonstrated to be pertinent to numerous necessities of vegetation status checking remembering appraisal and observing changes for shade biophysical properties, such as vegetation fraction (VF), Leaf Area Index (LAI), a small amount of consumed photosynthetically dynamic radiation, and net essential creation (Asrar et al., 1984). Most vegetation indexes join data contained in two spectral groups, red and NIR. Impressive exertion has been consumed in improving the Normalized Difference Vegetation Index (NDVI) and in growing new lists to repay both for the air (Kaufman and Tanre, 1992), and overhang foundation (Huete et al., 2002). This conduct forestalls the utilization of the NIR for the assessment of moderate to high vegetation cover in crops.

In the vegetation index calculation, there is still unsolved discussion on including only the visible spectrum or including other spectral bands for instance Near-infrared (NIR) band (Gitelson et al., 2002). The author of this research strongly believes that it is important to include NIR for vegetation indexes calculation. Because plants are very sensitive to red and NIR bands.

In total, hundreds of vegetation indices exist, among these Normalized Difference Vegetation Index (NDVI) is one. NDVI is the most used vegetation index. It is used to indicate the health of the green vegetation (Rouse Jr et al., 1973). For low biomass situations, normalized difference vegetation index works better (Viña et al., 2004). It is calculated by the normalized procedure. It is the ratio of the difference between the near-infrared and the red band. These band regions are the highest absorption and reflectance regions of chlorophyll (Rouse Jr et al., 1973). The value of this index ranges from -1 to 1. But any value less than zero is not vegetation.

However, there are few research conducted before. (Tlapakova, 2016) has visualized the condition of drainage systems, their maintenance, and their defects. The researcher utilized different data sources such as satellite imagery, maps from the archive, and digital database (eagri(LPIS)).

Samapriya (2013) researched Remote Sensing and Geographic Information System (GIS) applications for drainage detection and modelling in an agricultural watershed. The essential target

of this research includes outlining and approving the presence of subsurface drainage tiles in each cropland utilizing Remote Sensing and GIS strategies.

This study provides a new insight into the use of remote sensing techniques for evaluation of the performance of the drainage system using long term time-series data to increase the reliability of the result. It is use only NDVI technique as the main technique to determine the functionality of the drainage system. Based on an assumption, the plants' response to electromagnetic energy is related to the health status of the plant.

1.2 Statement of the problem

Agricultural lands are regularly drained by agricultural drainage systems (ADS) which are intended to permit simple transport of water from land and advantage horticulture and farming yield because of the diminished degree of water in the fields (Oosterbaan and Nijland, 1994). These ADS can be surface depletes and jettison that allow the water to pass on the surface and are classified as "surface drainage systems", or tile channels that permit the water to pass under the soil and are classified as "subsurface drainage systems". Both surface and subsurface frameworks channel into an inward low, the general water accessibility in the field or territory of interest, and into an outer or primary channel transport which ships the water to the source or riverine framework. Tile waste has expanded the proportion of subsurface to surface seepage making significant worry about the hydrologic outcomes brought about by these subsurface farming waste frameworks hence subsurface tile channel frameworks are the focal point of the current examination. The area data of these tile channel frameworks are restricted furthermore, the tile channel arrangement designs are unpredictable, making recognition of subsurface frameworks an important apparatus in the appraisal of field hydrology and agreement stream of water through these agrarian regions. This further improves the comprehension of stream directing for control and evaluation of water quality and amount boundaries in each rural watershed.

We are presently at the beginning of a period when we are going to need to discover efficient arrangements supporting the maintainable utilize of rural arrive which, next to other components, loses its beneficial capacity due to the diminishing usefulness of arriving waste. The current period is characterized by energetic climate alterations, with developing hydrological extremes such as seriously exuberant precipitation or long-lasting dry spells. The scenarios of climatic changes for

Central Europe (Brázdil et al., 2009) assume to discuss temperature increments, hoisted evapotranspiration (ET), and, subsequently, diminishes of summer cruel and negligible releases (Kulhavý and Fučík, 2015). Ready to see the negative impacts of these marvels as visit inundations, surges, erosive forms, or sensational drops of water asset supplies. This requires changes in the administration of water assets in arrange to upgrade amassing and maintenance of water, ideally as of now in soil or in reasonable watershed zones (Feldman, 2013), emphasizing moreover the significance, flexibility, and potential of the waste frameworks. In a few cases, the significance of seepage frameworks is rubbished or not satisfactorily acknowledged in the Czech Republic (CR) and overseas. In any case, appropriately kept up rural drainage system ought to be considered as a figure playing an imperative part in both food security and administration of water assets (Madramootoo et al., 2007).

Studies indicated that there is a problem with the drainage system of agricultural land in the Czech Republic. According to Kulhavý and Fučík (2015), the following two reasons lead to the drainage dysfunction.

a. The fragmented ownership of drained land may serve as an illustrative parallel to the negative effects of excessive fragmentation of land ownership that occurred after 1990 in Central and Eastern Europe, as shown by. Such a fragmentation profoundly hampers more complex forms of drainage system maintenance. This problem caused the second reason.
b. In the two last decades, consultations regarding land drainage or irrigation systems and state support of drainage system repairs and maintenance have practically been abolished. The subsidies for drainage repairs and maintenance were targeted at the owners of drainage systems as well as the farmers. However, the awareness and concern, especially of landowners, was regrettably low. On the other hand, the repairs were not done with adequate professional and financial support, and therefore the maintenance was neither effective nor durable (Kulhavý and Fučík, 2015).

The complexity of the natural conditions of CR along with the topological complexity of constructed drainage systems, as well as the overlay of older systems with the new ones, emphasizes the need for adequate detailed data primarily expressed in the project documentation.

To fully understand the scale of the problem and to act towards a solution it is important to exploit the currently available technology. Therefore, thesis this will explore the capability of remote sensing technique in identifying the extent of the problem in a short period of time with precision.

1.3 Objective of the study

The objective of the thesis is to evaluate the functionality of the controlled drainage systems in selected locality in the Czech Republic based on vegetation indexes using GIS analysis of satellite data. Select the suitable vegetation index/indices (after a careful review) and assess the extent of effect by controlled drainage.

1.4 Limitation of the study

The study was conducted with all possible efforts by controlling the limitation. It was planned to include satellite imageries for two years (2019 and 2020). Even though it was managed to download scenes for the two years. It wasn't possible to conduct the study for both years because of lack of water level data.

The other limitation was spatial resolution. The satellite image used for the analysis was freely downloaded. The resolution of the imageries was 10 meters. The information gathered could be of higher precision level if high resolution imagery is used.

2 Literature review

2.1 Remote sensing

Remote sensing is that the science and art of obtaining information about an object, area or phenomenon through an analysis of the information acquired by a tool which isn't involved with the article, area or phenomenon under investigation (Reddy, 2008). It's further required that such sensing is also achieved within the absence of any matter within the intervening space between the item and therefore the observer. Discussing of this, the data about an object, an area or any phenomenon must be available in a very form that may be impressed on a carrier vacuum. The information carrier, or the media, is electromagnetic energy. Remote sensing data basically consists of wavelength intensity information acquired by collecting the nonparticulate radiation leaving the item at specific wavelength and measuring its intensity.

2.2 Electromagnetic (EM) radiation

The tree we see as green, the sky as a blue and a red cross as a red is a result of sensation of colour caused by electromagnetic radiation. Red, Green and Blue relate to forms of energy which we commonly refer to as light (Janssen et al., 2001). Light is electromagnetic radiation that is visible to human eyes. For light based remote sensing the only source of light is Sun. So, it is the light reflected after reaching the surface is that help as identify the object. Light has two oscillating components; the energy constantly changes between electrical energy and magnetic energy (Janssen et al., 2001).

Since remote sensing is a bout interaction of electromagnetic radiation with a certain surface. It is important to discuss the model of EM radiation. EM radiation can be modelled in two ways: by waves of changing electric and magnetic fields or particles called photons. Photons are the origin of all energy. Because all matters at a temperature above absolute zero vibrates and emit some form of electromagnetic energy. So, temperature is a measurement of vibration energy released from the matter. Wave is an emitted or reflected energy traveling in a certain rate. Mostly wave of energy moves at the speed of light (300,000 m/s).

It is very important to discuss about wavelength when discussing the models of EM radiation. Because wavelength (λ) is a measurement of energy which is carried by the electromagnetic wave. Wavelength is measured from wave crest to wave crest or in an opposite way from trough to trough. So, the longer the wavelength the lower the frequency and the lower the energy (Dragotti and Gastpar, 2009). And vice versa, the shorter the wavelength the higher the frequency and the higher the energy it carries.

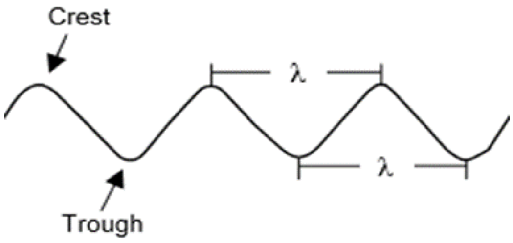

Figure 1: Electromagnetic wave morphology. Source*:* Dragotti and Gastpar (2009), Remote sensing application guide. pp 14

The electromagnetic wave is plotted from the short wave to longwave based on logarithmic scale called electromagnetic spectrum. The EM spectrum range from a cosmic ray which is the shortest wave to TV and radio waves which is the longest wave (Janssen et al., 2001). It must be noted that there is no clear boundary between each spectrum.

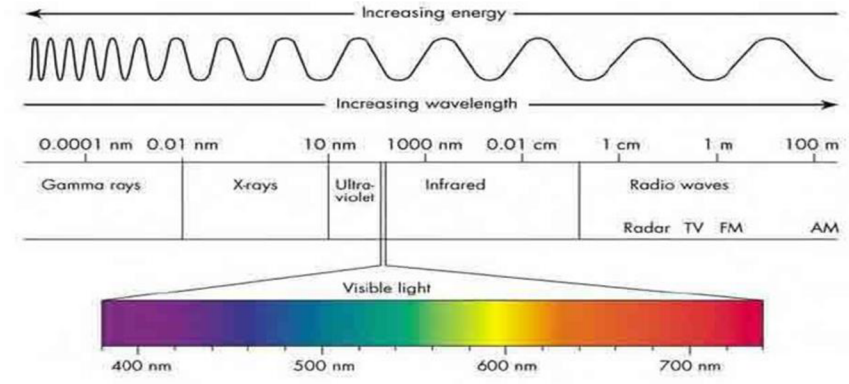

Figure 2: Electromagnetic spectrum. Source: Aggarwal, (2005), Application of Remote sensing. pp 28

Different part of the spectrum has different function in remote sensing. For this study the visible light (400 nm - 700 nm) and near infrared (800 nm - 2,500 nm) is used. The visible light is a composite of red, green, and blue bands. This part of the electromagnetic spectrum is used for passive remote sensing sensors.

2.3 Types of sensors

There are two types of remote sensing from the sensor's perspective: active remote sensing and passive remote sensing. An active remote sensing system generates and uses its own energy and records the reflected energy which carries the information about the target and/or the surface (Reddy, 2008). This type of system is very use full for part of the earth under permanent cloud cover and low sun angle. The typical example for this type of remote sensing system are Radar and Light Detection and Ranging (LIDAR)

Passive Remote sensing system is totally dependent on the solar electromagnetic radiation. It operates in a visible and infrared spectrum (Reddy, 2008). The appearance and characteristics of the target materials can be obtained from incident electromagnetic energy that is reflected, scattered, or emitted by these materials on the earth's surface and recorded by the passive sensor. The typical sensor for this type of remote sensing are film photography, infrared, charge-coupled devices, and radiometers. This system comprises two distinct processes called data accusation and data analysis.

2.4 Satellite imagery

On the perspective of sensor carrier there are two types of remote sensing platforms. They are air born based sensor and satellite-based system. The sensor in both systems can be either passive or active sensor. For this study the satellite platform is used. Because space borne system is currently used to support scientific researches (Schowengerdt, 2007). This system has gone through a long process since the starting point in 1972 (Schowengerdt, 2007).

The first satellite image collection has started at the time Landsat multispectral scanner system (MSS) provided in 1972. This satellite had the following characteristics: The sensors were multispectral band sensors, the highest spatial resolution was 80 meters, the repeating time was 18 days. The purpose of these satellite images ware general purpose (Schowengerdt, 2007).

After the starting of this system, there have been four additional MSS systems, two Thematic Mapper (TM) systems, and the Enhanced Thematic Mapper Plus (ETM+) in the Landsat series. There have also been five higher resolution French SPOT systems, several lower resolution Advanced Very-High-Resolution Radiometer (AVHRR) and Geostationary Operational

Environmental Satellite (GOES) systems, and National Aeronautics and Space Administration's (NASA) sensor suites on the Earth Observing System (EOS) Terra and Aqua satellites, as well as a wide variety of other multispectral sensors on aircraft and satellites (Schowengerdt, 2007). An illustration of some of these optical remote sensing systems in a performance space expressed by two key sensor parameters, the number of spectral bands and the ground sapling distance (Spatial Resolution). All the satellites are visualized on the figure 3 with the parameters.

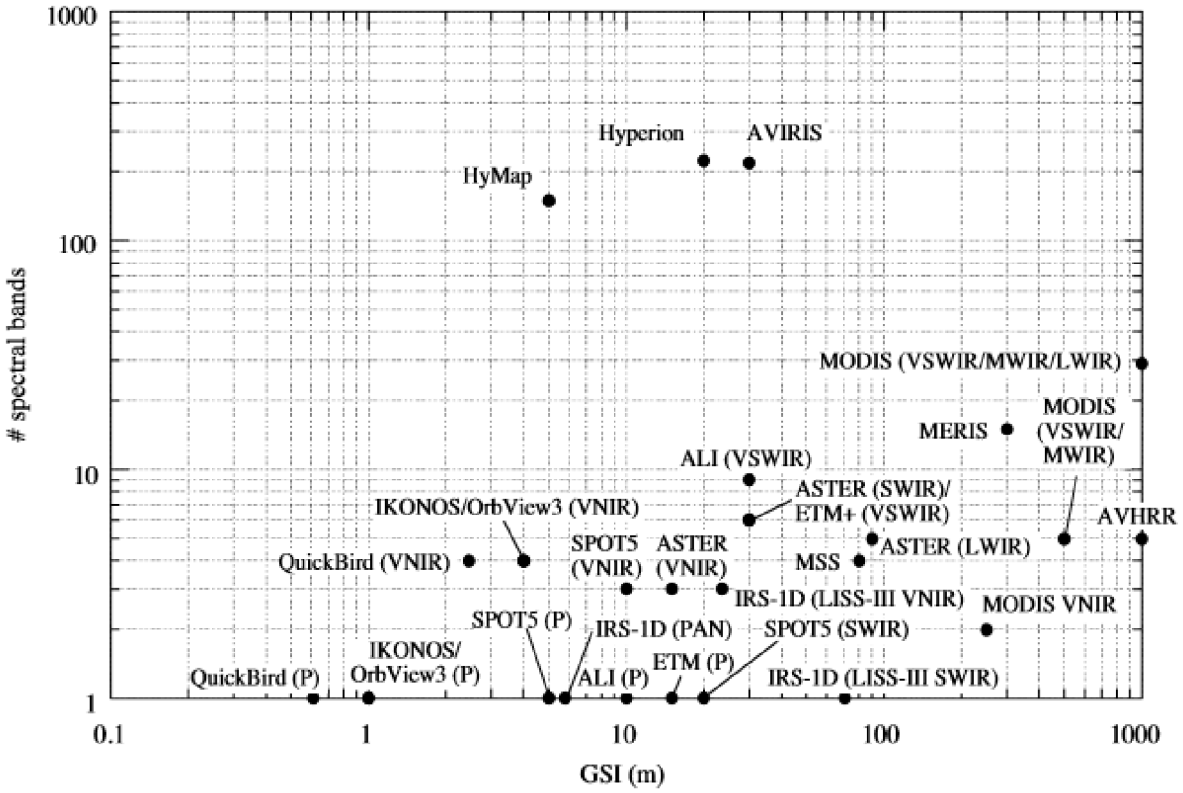

Figure 3: A plot of some remote-sensing systems in a two-dimensional parameter space. Source: Schowengerdt (2007), Remote Sensing: Models and Methods for Image Processing. pp 46

Many countries, including Canada, India, Israel, Japan, South Korea, and Taiwan, and multinational agencies such as the European Space Agency (ESA) now operate remote sensing systems. The European space agency has launched a mission called Sentinel-2 under Copernicus program (Copernicus, 2021). The main purpose of this mission is earth observation. The mission was a combination of twin satellites; sentinel-2A which is launched on 23 Jun 2015 and Sentinel-

2B which is launched on 7 March 2017 (Copernicus, 2021). The satellite collect image with spatial resolution of 10 m, 20 m, and 60 m. Sentinel-2 covers land surface from 56^{o} South to 84^{o} North. The satellites are equipped with multi spectral instrument that can sense 13 spectral channels in the visible/near infrared and short wave infrared spectral range.

The Sentinel-2 satellite data can be accessed for free on Earth observing system (EOS). The data is accessed for free because the Sentinel-2 mission has free and open data policy. Beside the raw imagery it is possible to access different types of vegetation indices. Which are very useful for different research purpose and crop monitoring.

EOS is a digital online platform which provide very suitable medium for searching, processing, and analysing huge quantity of satellite data. EOS is completely cloud based satellite imagery collection. Because of the advantages mentioned above it is used as source of data for this study topic.

2.5 Resolutions

Since the different remote sensing systems were discussed, it is important to discuss also about the characteristics that determine the quality and the usability of the product of the sensors. These characteristics are called resolution. In most literatures there are three types of resolution. These are spatial resolution, spectral resolution, and temporal resolution. But on some literatures, they add another type of resolution that is radiometric resolution (Reddy, 2008). Spatial resolution refers to the size of the smallest part that can be detected by a satellite sensor or displayed in a satellite image. It is determined by the sensor parameter and angle and height of the sensor. Spectral resolution refers to the ability of the satellite to measure specific wave lengths of electromagnetic spectrum. Temporal resolution is the time interval between sensing of certain area.

2.6 Vegetation indices (VI)

Vegetation has a distinct spectral signature from other land cover and land use type. This is due to the chlorophyll content of vegetations. Vegetations absorb the red and blue band due to the pigments such as chlorophyll which reside in the upper layer of the leaf. In contrast there is strong reflectance at near infrared region, caused by scattering in spongy mesophyll (Devitt et al., 2018).

Many techniques are formulated to analysis vegetations quantitatively from satellite image. One of these techniques are Vegetation indices. The vegetation index concept was developed as a method of reducing the number of variables present in multispectral measurements down to one unique parameter (Devitt et al., 2018). VI is used as a tool in land cover classification, climate and land use change detection, drought monitoring, and habitat loss are the few.

Vegetation indices (VIs) to monitor terrestrial landscapes from satellite sensors were first developed in the 1970s and have been highly successful in assessing vegetation condition, foliage, cover, phenology, and processes such as evapotranspiration (ET) and primary productivity (Pettorelli et al., 2005). VIs are robust satellite data products computed the same way across all pixels in time and space, regardless of surface conditions. As ratios, they can be easily cross-calibrated across sensor systems, ensuring continuity of data sets for long-term monitoring of the land surface and climate-related processes.

2.6.1 Basic vegetation indices

2.6.1.1 Ratio vegetation index (RVI)

Ratio Vegetation Index (RVI) is the simplest vegetation index. It is proposed in 1969 as one of the first VI. RVI is simply the ratio of near infrared and red band. The logic of this index is, leaves absorb relatively more red than infrared light (Xue and Su, 2017). The larger the ratio implies the healthy the vegetation is.

Eq 1 $$RVI = R / NIR$$

This index gives general indications of vegetation. The disadvantage of this index is: - one if the reflectance for the red band is zero it is impossible to produce the index value for this pixel. Two there might be a wide range of values depending on the amount of red reflectance (Sneha et al., 2012). The RVI is widely used for green biomass estimations and monitoring, specifically, at high density vegetation coverage, since this index is very sensitive to vegetation and has a good correlation with plant biomass. However, when the vegetation cover is sparse (less than 50% cover), RVI is sensitive to atmospheric effects, and their representation of biomass is weak.

2.6.1.2 The difference vegetation index (DVI)

This vegetation index is the difference of near infrared and red band. It is a good indicator for vegetation development. It has a better capability for time-based vegetation status and condition (Richardson, 1978). The DVI is very sensitive to changes in soil background; it can be applied to monitoring the vegetation ecological environment. Thus, DVI is also called Environmental Vegetation Index (EVI) (Xue and Su, 2017). It does not account for the difference between reflectance and radiance caused by atmospheric effects or shadows.

Eq 2 $$DVI = NIR - R$$

2.6.1.3 The perpendicular vegetation index (PVI)

This vegetation index is based on a logic of the response of near infrared (NIR) and red band and the soil line. The distance between the point of reflectivity and the soil line has been defined as the perpendicular vegetation index. PVI is very efficient in removing the effect of soil background. Unlike the other simple vegetation index PVI has low sensitivity to atmospheric effects. It is useful for leaf area calculation, vegetation classification and identification. The weakness of this vegetation index is its sensitivity for soil brightness.

Eq 3 $$PVI = \sqrt{(\rho soil - \rho veg)2\ R - (\rho soil - \rho veg)2NIR}$$

where ρsoil is the soil reflectance; ρveg is the vegetation reflectivity

2.6.1.4 Normalized difference vegetation index (NDVI)

Normalized Difference Vegetation Index is the highly used vegetation index. It is calculated by normalized procedure. It is the ratio of the difference between near infrared and red band. These band regions are the highest absorption and reflectance region of chlorophyll. It is used to indicate the health of the green vegetation (Rouse Jr et al., 1973). For low biomass situation normalized difference VI work better (Henebry, 2004). The weakness of this index is its sensitivity to the effect of soil brightness, soil colour, atmosphere, cloud and cloud shadow. It requires the atmospheric correction of satellite images (Xue and Su, 2017).

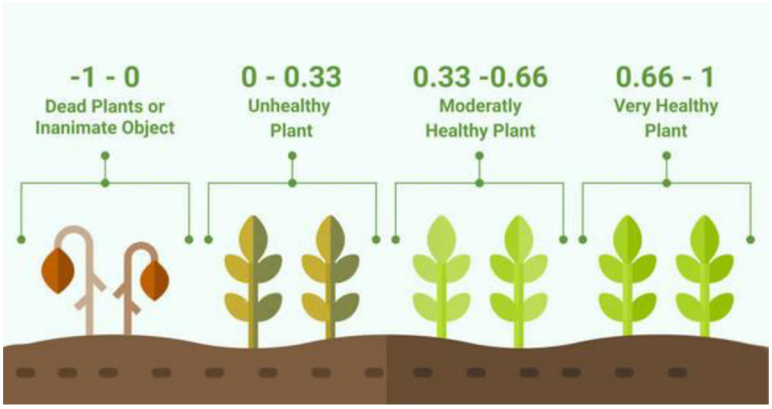

Figure 4: NDVI value categorization. Source: https://eos.com/wpcontent/uploads/2020/07/plants.jpg

The value of this index ranges from -1 to 1. But any value less than zero is not a vegetation. Positive Smaller values that are closer to zero (0.2 to 0.4) represent shrub and grassland. Vegetations are mostly between 0.2-0.8. For low biomass situation normalized difference VI work better (Shedekar et al., 2017)

Eq 4
$$NDVI = \frac{(NIR - Red)}{(NIR + Red)}$$

For Sentinel-2 Near Infrared is represented by Band 8 (B8) and Red is represented by Band 4 (B4). The formula for NDVI in Sentinel-2 dataset is described as follow.

Eq 5
$$NDVI = \frac{(B8 - B4)}{(B8 + B4)}$$

2.6.1.5 Wide dynamic range vegetation index (WDRVI)

This index is comparable to NDVI, but it uses a weighting coefficient (a) to cut back the disparity between the contributions of the near-infrared and red signals to the NDVI (Gitelson , 2004). This modified vegetation index is proposed to fix the limitation of NDVI in the case of moderate and high vegetation cover. The WDRVI is especially effective in images that have moderate-to-high vegetation density when NDVI exceeds 0.6. Henebry et al. (2004) mentioned on their study that the recommended weighting coefficient value is 0.2.

Eq 6
$$WDRVI = \frac{(\alpha * NIR - Red)}{(\alpha * NIR + Red)}$$

ɑ = weighting coefficient, it ranges from 0.1 to 0.2

2.6.2 Vegetation indices considering atmospheric effects

2.6.2.1 Atmospherically resistant vegetation index (ARVI)

ARVI was first proposed and developed to analyses vegetation from the Earth Observing System (EOS) Moderate Resolution Imaging Spectroradiometer (MODIS) sensor. This index is formulated based on the understanding that the atmosphere influence mainly Red (R) band compared to the Near Infrared (NIR). The atmospheric effect on the red channel is corrected using the difference in the radiance between the blue and the red channels. ARVI is useful to minimize the effect of moderate to small size aerosol particle (Gitelson et al., 2002). Unlike the other indexes atmospheric resistant vegetation index is more dependable to overcome topographic effect.

Eq 7
$$ARVI = \frac{(NIR - RB)}{(NIR + RB)}$$

Where RB is the difference between Red (R) and Blue (B) channel.

2.6.2.2 Visible atmospherically resistant index (VARI)

This index is based on the theoretical background to predict the part of vegetation in an image that has minimum sensitivity to atmospheric effect. Atmospheric resistant vegetation index is the foundation for VARI (Gitelson et al., 2002). In the analysis only the visible fraction of the spectrum is used. It is best for multispectral (RGB) scenes.

Eq 8
$$VARI = \frac{(Green - Red)}{(NGreen + Red - Blue)}$$

2.6.2.3 Enhanced vegetation index (EVI)

Enhanced vegetation index is first proposed for the use of Moderate Resolution Imaging Spectroradiometer (MODIS) data as an improvement over NDVI by maximizing the vegetation signal in area of high leaf area index (LAI). EVI uses the Blue channel to remove the soil background signal and minimize atmospheric influence (Huete et al., 2002). As same as NDVI

value EVI value range from -1 to 1. The reflectance value for healthy vegetation ranges from 0.2 to 0.8. It is advisable to use this index in the area with high chlorophyll. But unlike the Atmospheric resistant vegetation index (ARVI) it is highly affected by topography.

Eq 9 $$EVI = 2.5 * \frac{(NIR - Red)}{\big((NIR) + (C1 * Red) - (C2 * Blue) + L\big)}$$

The general formula of EVI indicated above has coefficient C1 and C2 which are used to adjust atmospheric scattering. The L value is used to correct soil and canopy background. The most common number used in place of this coefficients are C1=6, C2=7.5 and L=1. The numbers are commonly used by NASA. It is proposed to avoid confusion what number to use in calculating Enhanced Vegetation Index.

Eq 10 $$EVI = 2.5 * \frac{(NIR - Red)}{(NIR + 6 * RED - 7.5 * Blue + 1)}$$

2.6.3 Vegetation indices considering background soil effects

2.6.3.1 Soil adjusted vegetation index (SAVI)

Soil Adjusted Vegetation Index is relatively like Normalized Difference vegetation Index. The difference between the two indexes is the suppression of the soil pixels in the case of SAVI. The creator of this index (Qi et al., 1994) included soil adjusted factor or soil conditioning index (L) to the formula of NDVI. To minimize the influence of soil noise on the result of the vegetation index.

Eq 11 $$SAVI = \frac{(NIR - Red)}{(NIR + RED + L)} * (1 + L)$$

or

Eq 12 $$SAVI = \frac{1.5 * (NIR - Red)}{(NIR + RED + 0.5)}$$

The range of L is from 0 to 1. Based on empirical understanding the value of L is dependent on specific environmental condition. When the amount of plant coverage is high the coefficient number close to 1, implying the soil background has less or no effect on the information gathered about the vegetations (Xue and Su, 2017). But this is a very theoretical condition that rarely exist in the real situation (Gitelson et al., 2002). The L value is set to “0” in the case SAVI will be same

to NDVI. For the optimum adjustment of the soil influence on the result it is recommendable to use the L factor in reverse way to the plant coverage. It is recommendable to use this index for analysis of young crops for instance for arid regions with sparse vegetation.

There are new versions of Soil Adjusted Vegetation Index (SAVI). Which are described as SAVI2, SAVI3 and SAVI4. These versions are developed based on the logical background to consider the effect of wet and dry soil (Rondeaux et al., 1996).

2.6.3.2 Modified soil adjusted vegetation index 2 (MSAVI2)

This index is the improved version of the soil adjusted vegetation index. It simplifies modified soil adjusted vegetation index (MSAVI). It minimizes soil noise and maximize the vegetation signal range. The MSAVI2 based on an inductive method that does not use the constant soil adjustment factor (L) value to minimize the effect of soil reflectance. It uses the self-adjustment L factor. The self-adjusted vegetation index allows to automatically adjust the L value to the appropriate the first one requires knowledge about the vegetation (Qi et al., 1994).

Eq 13

$$MSAVI2 = \frac{2 * NIR + 1 - \sqrt{(2 * NIR + 1)^2 - 8(NIR - Red}}{2}$$

2.6.3.3 Optimized soil adjusted vegetation index (OSAVI)

This index is primarily planned to optimize the influence of soil radiance on the result of soil adjusted vegetation index (SAVI). It uses a value 0.16 for the canopy adjustment factor. The canopy adjustment factor value is the variance of the result of comparison among NDVI, SAVI, MSAVI, TSAVI (Transformed Soil-Adjusted Vegetation Index) and GEMI (Global Environmental Monitoring Index). This Vegetation index can be used for both at high and low vegetation cover. But it will be at its best when it is used in the case of sparse vegetation cover where the soil is visible through the canopy (Rondeaux et al., 1996).

Eq 14

$$OSAVI = \frac{(NIR - Red)}{(NIR + RED + 0.16)}$$

2.6.4 Vegetation indices common on (EOS) platform

The Earth observing system platform has more than twenty indices that can be accessed for free. Most of them are analysed based on the visible and near infrared and some based on spectral values beyond that (e.g., Land/water Index and Healthy Vegetation index). Some of the vegetation indices that are note discussed under any category are presented below.

2.6.4.1 Green chlorophyll index (GCI)

GCI estimate the content of leaf chlorophyll to describe the physiological state of plants. It is applicable to wide varieties of plant species. Having broad near infrared and green spectral band provides a better prediction of chlorophyll content while allowing for more sensitivity and a higher signal-to-noise ratio (Gitelson et al., 2003). The index is best to visualize the impact of seasonal variation on plants situation.

Eq 15

$$GCI = \frac{(NIR)}{(Green)} - 1$$

2.6.4.2 Structure insensitive pigment index (SIPI)

The Structure Insensitive Pigment Index is good for analysis of vegetation with the variable canopy structure. It diminishes the impact of the variable canopy structure, while optimizing sensitivity to the bulk carotenoids to chlorophyll ratio. It estimates the ratio of carotenoids to chlorophyll: the increased value signals of stressed vegetation. It is best applicable for monitoring plant health in regions with high variability in canopy structure or leaf area index, for early detection of plant disease or other causes of stress. The value ranges from 0 to 2, where green vegetation is represented from 0.8 to 1.8 (Gitelson et al., 2003).

Eq 16

$$SIPI = \frac{NIR - Blue}{NIR - Red}$$

To conclude the topic about vegetation index, it has been made to include most of the vegetation indices that are relevant with the study. But it has to be clear that there are hundreds of vegetation indices. Some are based on profound theoretical background, and some are just on the level of experiment.

2.7 Agricultural water management

2.7.1 Irrigation

Appropriate irrigation system must be implemented to maximize the effect of the farm input and additionally to helps the farmer get more yield. It is obvious that water is a renewable resource but because of the population pressure on earth water is becoming a very scares resource. So, the inaccessibility of water is threatening agricultural productivity (Shao et al., 2015).

There must be a way to overcome this problem while maintaining and or maximizing the yield. For this problem one big solution is applying controlled irrigation. Controlled irrigation is water wise pre-planting and after-planting practice. It is about how to alternate wetting and drying of a crop safely during the crop growing period.

2.7.2 Drainage

In agricultural water management the focus is the basic principles and theories of drainage is the removal of excess water from agricultural land. Draining excess water is important because the excess water in the soil hinder the penetration crops root. The excess water reduces the activity of microorganisms by reducing the availability of oxygen(USDA, 1974). Additionally, the excess water highly affects the soil structure. Applying drainage system on agricultural field will help to minimize all the above problems. Additional it give an advantage to reduce salinity caused by capillary rise (Ritzema, 2007). There are two major types of drainage systems Surface drainage system and subsurface drainage system (USDA, 1974).

2.7.2.1 Surface drainage system

The surface drainage system is a method of removing water from the agricultural land directly by smoothing, land levelling, bedding, and ditching. Subsurface drainage system work by installing buried collectors below the ground (USDA, 1974). This method is very technique for the humid and sub-humid zones. Surface drainage is applied on soils with low permeability, soils with a small permeable layer, impermeable layer between 2.5 and 6 meters, uneven ground surface with pockets or rugged topography that delay or avoid natural runoff, and as a supplement to subsurface drainage (Hasić and Matula, 2020).

2.7.2.2 Subsurface drainage system

On the other hand, Subsurface drainage system are typically introduced to make a control of the ground level water. There are numerous benefits of subsurface drainage, entomb alia, air circulation to root zone, improvement of soil construction and support of soil temperature, farm machine functionality, evacuation of huge measure of salts from the root zone, no control of surface land, little (Ritzema, 2007). Nonetheless, a few drawbacks can be recognized too, like significant expenses for construction, need for more steeper slope gradient, development, and fix costs.

2.7.3 Components of drainage system

The first and major component of drainage system are pipes. Drainage pipes can be made up off polyvinyl chloride (PVC), vitrified clay, iron, concrete, iron, and asbestos. The other major component of drainage system is bedding. Bedding is a safety appliance to protect the pipeline from excessive load. Additionally, the bedding helps to place the pipeline in a steady gradient (Feldman, 2013). The controlling components of drainage system are regulation points. The control centres serve to maintain the water level or the discharge at the desired level. These control points can be operated manually by human operator or by the water forces on a hydro-mechanical gate, by a float with programmable logic controller (PLC) of an electro-mechanical gate (Sneha et al., 2012). Drainage regulation points are mostly supply oriented control system (Richard, 2006).

2.7.4 Designs of drainage system

Design of drainage system varies depending on the topography of the drained area, sources of excess water, and other field conditions. According to the USDA engineering field handbook the drainage system design categorized into three types.

(a) **Random system**: - A random field drainage system is used where the topography is undulating or rolling and has isolated wet areas. The main drain is generally placed in the lowest natural depression, and smaller drains branch off to tap the wet areas (USDA, 1974).

(b) **Parallel system**: - The parallel field drainage system consists of laterals that are perpendicular to the main drain. Variations of this system are often used with other patterns. In many cases, the parallel system is desirable because it provides intensive drainage of a given field or area (USDA, 1974).

(c) **Herringbone system**: - The herringbone field drainage system consists of laterals that enter the main drain at an angle, generally from both sides. If site conditions permit, this system can be used in place of the parallel system. It can also be used where the main is located on the major slope and the lateral grade is obtained by angling the laterals upslope (USDA, 1974).

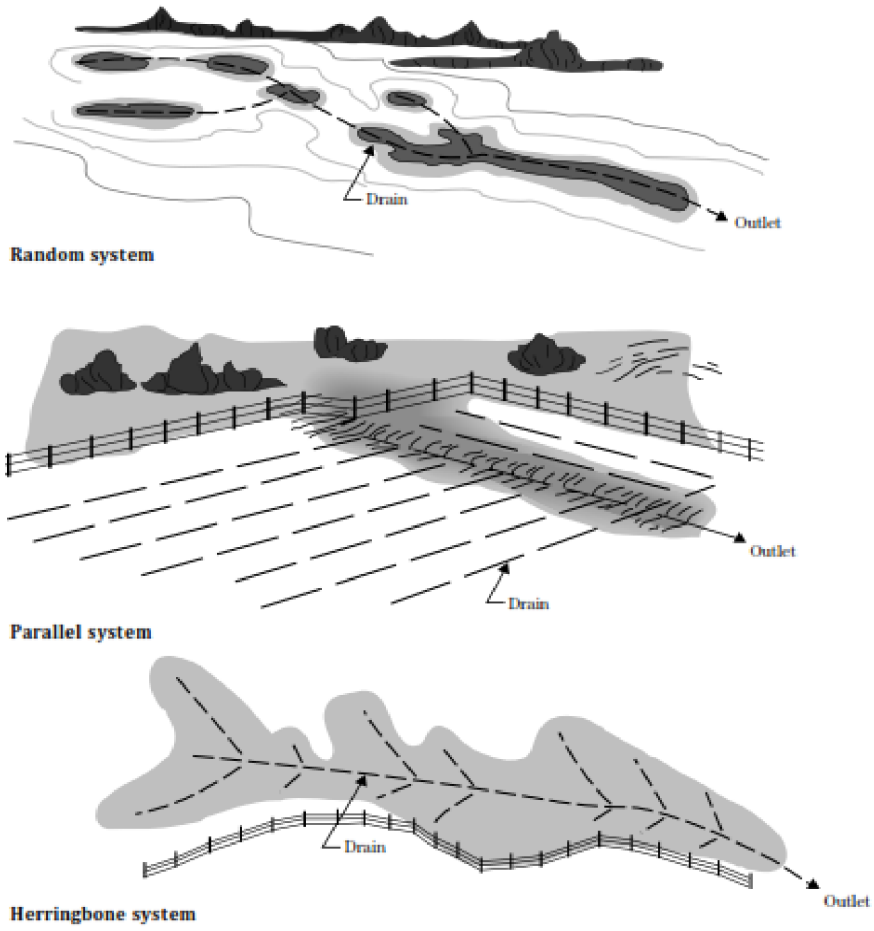

Figure 5: Types of Drainage designs. Source: Shedekar et al., (2017). GIS and GPS Applications for Planning, Design and Management of Drainage Systems. pp. 4

2.7.5 Controlled drainage

Controlled drainage system is a very useful sustainable water management method (Hasić and Matula, 2020). This method is applied to avoid all drawbacks of the conventional drainage system (Hasić and Matula, 2020). Controlled drainage system can be either surface or subsurface drainage system. The Surface Controlled drainage system is applied by constructing flashboard riser along

the water ditch. The flashboard functions to control the drained flowing water. In the case of subsurface controlled drainage system, the drainage inline control structure install below the surface (Liu et al., 2019).

From the agricultural point of view, controlled drainage system is agricultural land water management system which protect nutrient lose due to erosion and flooding. In addition, it helps agricultural land drained as required to minimize the effect of over flooding on crops and to keep the water table of the soil in the plants root zone (Liu et al., 2019). The controlled drainage system allows the water level to be artificially set in the field.

To define controlled drainage from functional perspective; controlled drainage systems are used to reclaim and/or conserve land for farming, to maximize crop production per season and to utilize the farmland more than once in a year. The controlled drainage system is also useful to use the farmland for more than one crop type (Oosterbaan et al., 1994). Oosterbaan suggested that the installation of a subsurface drainage system has generally two direct effects and many indirect effects. The most complicated objectives are the indirect objectives.

The direct effects of installing a drainage system are:

a. A reduction in the average amount of water stored on or in the soil, inducing drier soil conditions and reducing water logging.
b. A discharge of water through the system.
c. It minimizes the amount chemicals and/or fertilizers which are added by the farmer not to contaminate down slope area.
d. To intercept water flowing from adjacent highland.
e. Management of a ground water table to maintain proper soil moisture for optimum plant growth, to sustain or improve water quality, and to conserve water (USDA, 2001).

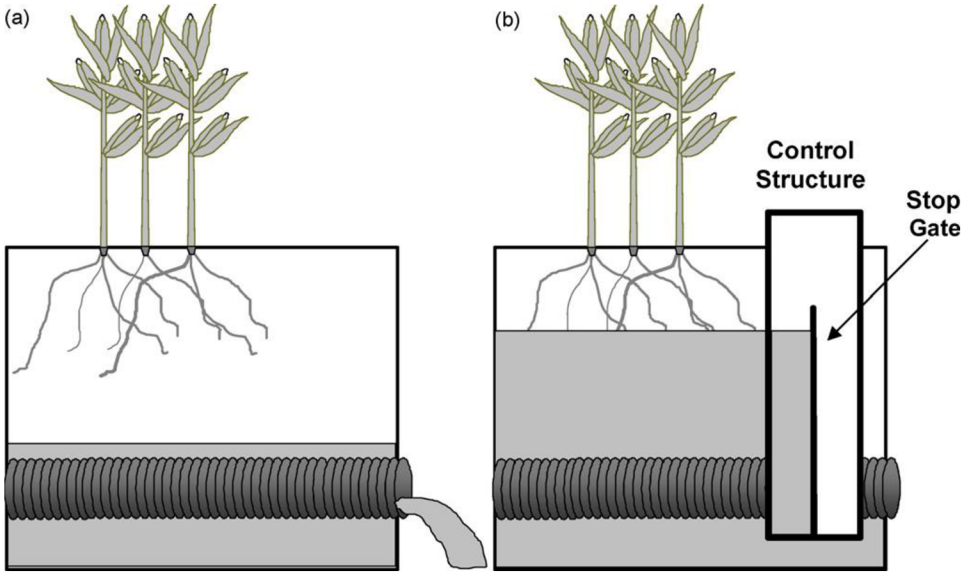

Figure 6: Schematic of (a) conventional or uncontrolled tile drainage (UCTD); and (b) controlled tile drainage (CD). To help mitigate waterlogging damage to crops, the water flow control structure will allow drainage waters to pour over the control structure stop gates (dam) if water table heights exceed the stop gate level. Source: Corinne, (2018). Sustainable Sanitation and Water Management Toolbox.

The placement of drainage control is not random; it must be placed in a strategic drainage outlet of the farm. This result for the regulated water flow from the drainage system in the outlet. There are two types of drainage control structures. The first one is open ditch flashboard riser structure, and the second type of structure is an inline control structure that is attached directly to subsurface drainage pipe.

2.7.6 Dysfunctionality of drainage system

The correct functionality of drainage system is determined by correct diagnoses of the wet area (USDA, 1974.). The dysfunctionality of drainage system arises because of so many reasons. The problems can occur both on subsurface and surface drainage system. On this review the dysfunctionality issues that could occur on subsurface drainage system is discussed. Because subsurface drainage system is the study issue of this study.

Farmland will in general be ineffectively depleted, especially where the subsoil penetrability is minimal. There are many wet regions, be that as it may, where there is no apparent association between the space of leakage, or a highwater table, and the topography of the area. High water

tables may happen where the soil is either gradually or quickly porous, where the environment is either muggy or dry, and where the land is either inclining or level (USDA, 1974).

The following are the cause for the dysfunctionality of drainage system. These are drainage system containing an opening between consecutive lines, absolutely unhampered drainage pipe; a totally blocked drainage pipe, stopped close to its midpoint; a soil filled drainage pipe; and a cut off or incompletely impeded drainage pipe (Borrelli et al., 2021).

2.7.7 Agricultural land drainage in Czech Republic

The total area of agricultural land in the Czech Republic (CR) is 4.2 million hectares (Hasić and Matula, 2020) . Most of the agrarian land is covered with arable land where individual yields are rotated (3 million hectares), permanent cultures (978 thousand hectares), gardens (209 thousand hectares), grape plantations (19 thousand hectares) and hop fields (10 thousand hectares) (Hasić and Matula, 2020).

In the CR, installation of drainage systems started in the second half of the 19th century. At that time, an exact engineering approach was applied, which proposed principles for drain spacing and depths in mineral agricultural soils based on foreign and domestic experience. However, the most part of Czech agricultural drainage systems was built in the 20th century, during three discrete periods. The first part was conducted before the first world war. The second period was in between the world wars. The third and the biggest part was built from 1960 to 1980 G.C. During the first two periods the construction was supported by the government and farmers association. In the CR more than 1,078,000 ha of agricultural land is covered with agricultural drainage system. After 1989 following the change on related ownership properties the maintenance and management of drainage systems becoming problematic. In this era inadequate or absent maintenance and repairs of these systems began and it resulted various degrees of degradation with adverse effects on the drainage systems functionality (Tlapáková, 2017).

The unproper management of the system is resulting agriculturally unfavourable situations. These situations clearly manifested by drainage water accumulation, waterlogging of the partially drained parcel. To combat this problem, it is important to have a precise data to know where and to what extent the problem is.

2.8 Remote sensing and drainage system

In this part, it has been reviewed and discussed some related works on assessment of the function of controlled drainage using satellite data. The drainage performance assessment is conducted from the point of view of methodology used for assessment.

Novakova et al. (2013) suggested that subsurface drainage systems can be spotted, and their performance examined using two major methods. These methods can be named as destructive and non-destructive methods. The destructive method is direct manual or machine-operated uncovering of the drainage. The non-destructive method is based on indirect methods for instance electric resistance, sonic, electromagnetic, and biological. According to Tlapáková (2017) the best non destructive method to identify and assess the performance of drainage system is remote sensing. She supported her argument saying that spatial hydro-indicative associations among the topography, vegetation, relief predisposition, soil etc. are the means for identification. And, she added information about the drainage system which can be obtained from the land parcel information system (LPIS) of eAGRI portal.

Krusinger (1971) presented that the identification of drainage system can be made by remote sensing method by analysing the difference in temperature, vegetation condition, vitality, and moisture (Tlapáková, 2017).

2.8.1 Remote sensing methods for identification of drainage system

The indirect interpretative method on a Phyto-designation principle has an efficiency 75-90% of areal covered. This principle utilizes the dissimilarity in plant growth as the dominant effect of drainage. The drain effect appears as a line in many cases clearly distinct in the image.

Samapriya (2013) on his research titled remote sensing and GIS for drainage detection and modelling; he clearly explained the remote sensing approach in the following way. The remote sensing method is very efficient to analyst large area in small amount of time. The remote sensing technique easily depict the efficient drainage system by the radiation response of the soil surface. Because the soil over efficiently drained drainage system should dry faster than the soil over malfunctioned system.

Samapriya (2013) used coloured infrared SPOT satellite images for analysis. Because the Infrared electromagnetic spectrum is very sensitive for soil moisture. He also tried to analysis the soil texture reflectance value. By stablishing relationship between soil texture and reflectance value. The stablished relationship is coarse, sandy soils which are well drained tend to have higher reflectance values than poorly drained fine textured soils.

Tlapáková (2017) conducted research titled "Agricultural drainage systems in the Czech landscape - identification and functionality assessment by means of remote sensing". Her work was totally focused on using the satellite imagery to identify the existence the drainage system and its functionality. Her assumption was if the drainage system is not properly functional; there will be detectable water accumulation on the land and/or soil erosion caused by water. She was trying to identify the drainage lines in the subsurface. Since it is not possible to detect subsurface object using standard remote sensing system. She tried to identify it through indirect system. By conducting hydro-indicative associations within relief, soil, and water.

The study presented in this thesis is completely different to the above reviewed studies in different aspects. The study is conducted in small agricultural parcel. It is in central Bohemia region at Strašov. None of the above reviewed studies has used a data for a long time to determine the functionality of the drainage system. Rather they tried to make direct measurement. The data source for this study is Land viewer from Earth observing system web platform.

This study will bring a new insight to the data utilisation originating from remote sensing technique in order to evaluate the functionality and performance of the drainage system.

2.8.2 Remote sensing for drainage assessment

Remote sensing (RS) images were not initially used to study the under-surface phenomenon. In the field of natural resources management RS images were initially used to evaluate the nearby wetness changes in land surface mapping. This strategy assumes the impact of line drainage pipelines on the drying-out of the piece of the soil profile over the channel, set apart with a shaded sign on the RS images. These signs depend on nearby changes in soil heat conductivity (Ritzema, 2007). Acquiring the whole information from remotely sensed imagery through visual image interpretation only is not possible. To acquire a detailed information from an image, different measurement techniques are designed. One of them is NDVI. NDVI is the most used to measure

vegetation index. Which is based on difference in plants absorption and reflection features of red (RED) and near-infrared (NIR) band.

The NDVI vegetation index is selected because plants are very sensitive for red and NIR wave bands. A physiological change of plants can easily be observed by the red and NIR band signature of plants. If plants are reflecting red band of solar radiation the plants are not processing photosynthesis. This indicates that the plant biomass is under a stress. For the above stated reasons, assessing the functionality and effect of the existing controlled drainage system is carried out by means of NDVI evaluation.

3 Materials and Methods

To achieve the general and specific objectives of the research, the following methodology has been used.

3.1 Description of the study area

The study area Strašov is about 100 km east of Prague, in the Pardubice district (Figure 7). It is part of about 250 ha area, where a drainage system was built in the 1980s. It is a relatively flat at an altitude from 210 to 220 m a.s.l. with mean annual temperature of 8-9°C and mean annual precipitation of 550-650 mm. Distribution of the precipitation and temperature variations during the experimental year of 2020 in comparison with the 5-year averages are displayed in Figure 8. The detailed elevation map with indication of the NDVI sampling points is displayed in Figure 9.

It is a relatively heterogeneous locality, where soils of different textures are found: i) in the southern part of the field, two different sorts of Phaeozems (control drainage affected area in this study) with the sandy clay loam texture and relatively high organic matter content with very low infiltration capacity are present, ii) in the middle part of the field up to the northern end, Stagnosols with low infiltration capacity are present while Stagnosols at the eastern end of the field were of clayey texture due to higher content of clay particles, iii) in the middle part (around the trees in Figure 7) Regosols with sandy texture composed of almost purely from sand and gravel were present. Saturated hydraulic conductivity values and dry bulk density values measured by DWR CULS Prague ranged from approx. 1 to 1000 cm/day and 1.22 to 1.70 g/cm^3 respectively (Kulhavý et al., 2020).

In autumn 2019 the soil was ploughed and in spring 2020 the sunflower crop has been seeded. After the sunflower harvest, the winter wheat has been seeded in no-tillage procedure for year 2021.

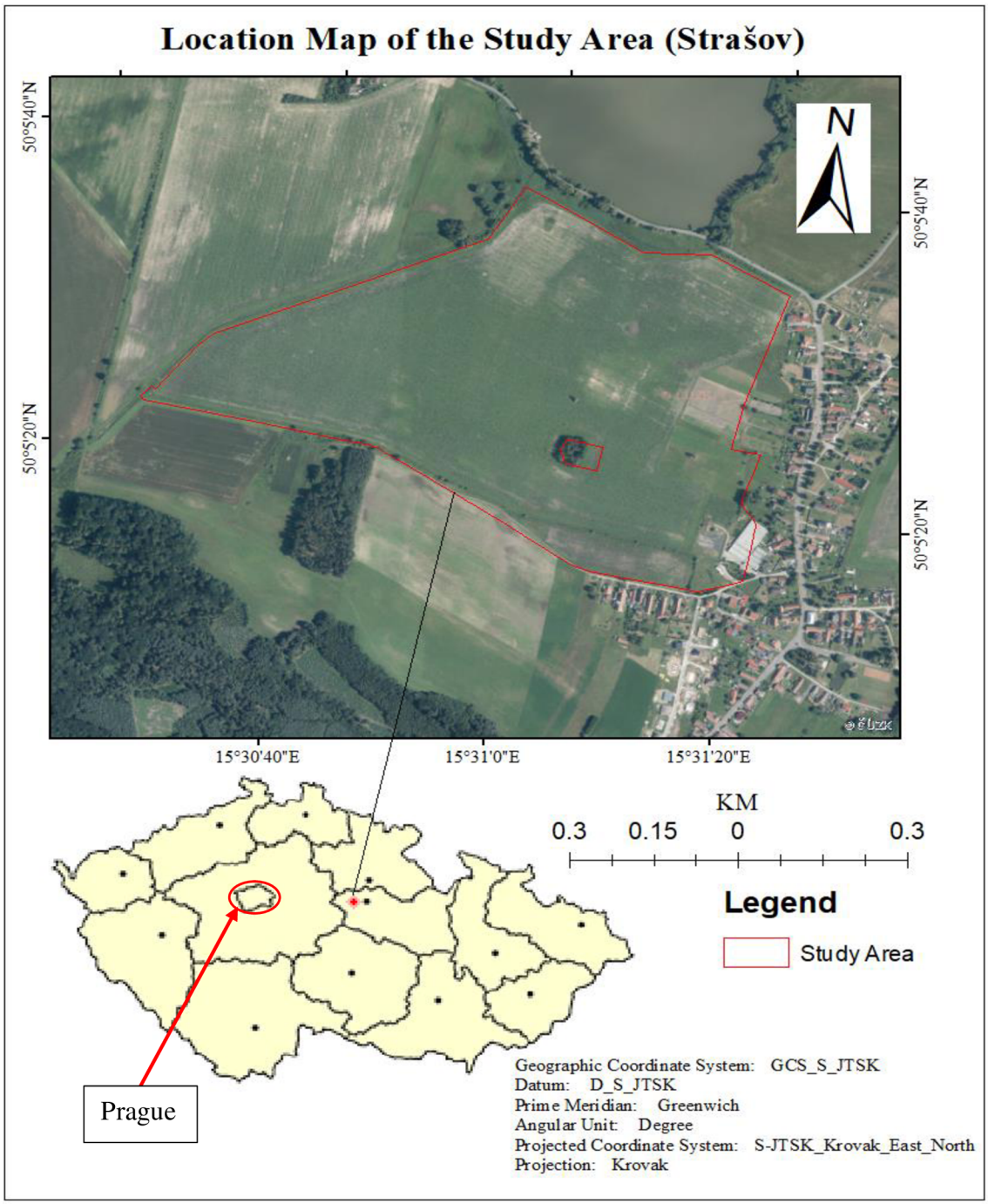

Figure 7: Location map of Strašov. Source: ArcGIS web map as modified by the author

The precipitation and temperature data for the analysis purpose is acquired from The Czech Hydrometeorological Institute (CHMI) (Český hydrometeorologický ústav (ČHMÚ)). The data is collected from Radovesnice II (Středočeský kraj, okres (district) Kolín) meteorological station.

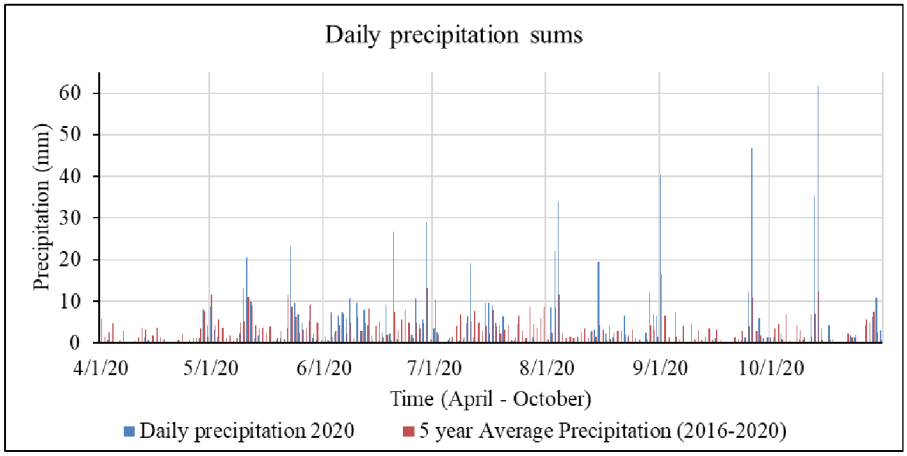

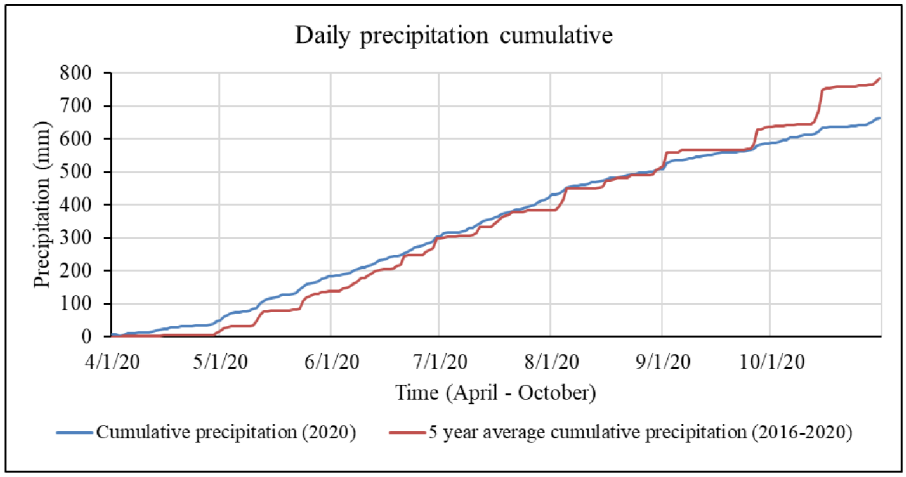

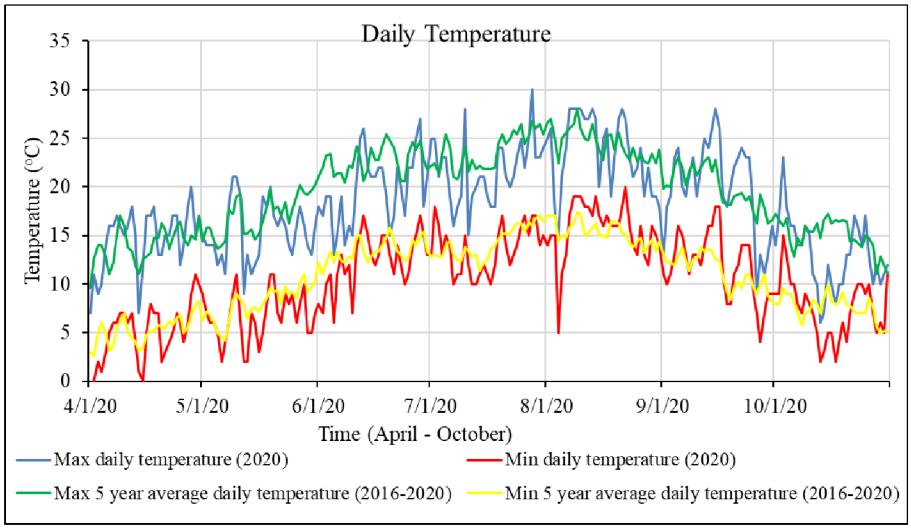

Figure 8: Long-term (2016-2020) meteorological data with indication of the values in 2020. Source: EOS, Land Viewer

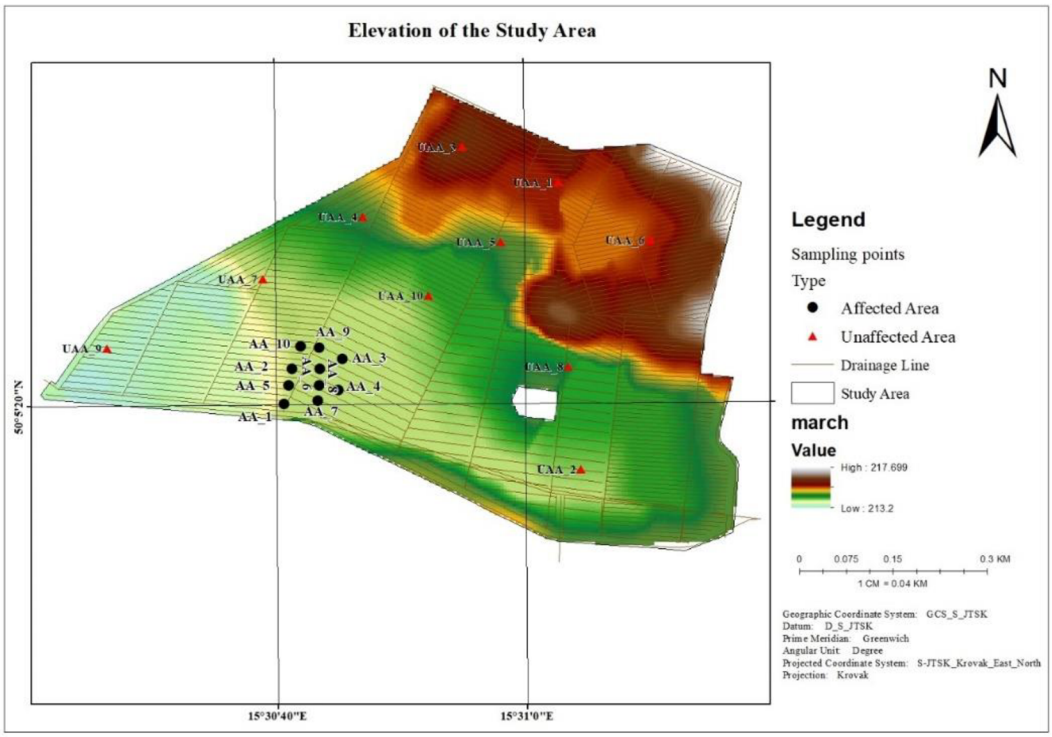

Figure 9: Topographic map of the study area; minimum elevation 213.19 m a.s.l., and maximum elevation 217.7 m a.s.l.

3.2 Research design

The study evaluates applicability of NDVI to assess the functionality and effect of the controlled drainage system on the study area. The study correlates the status of water level within the drainage system and the value of NDVI for predefined sapling polygons of the study area. Higher NDVI values in the dry period for the area affected by controlled drainage in comparison to the unaffected area, together with lower variation of NDVI values in periods rich on precipitation indicate the that the system is functional and can be evaluated. If the NDVI values for the affected area in dry periods are not bigger than for the unaffected area, pure or no function of the system would be identified.

The process of assessing the functionality of the existing controlled drainage system has different components. The overall workflow of the research is described on the (Figure 10).

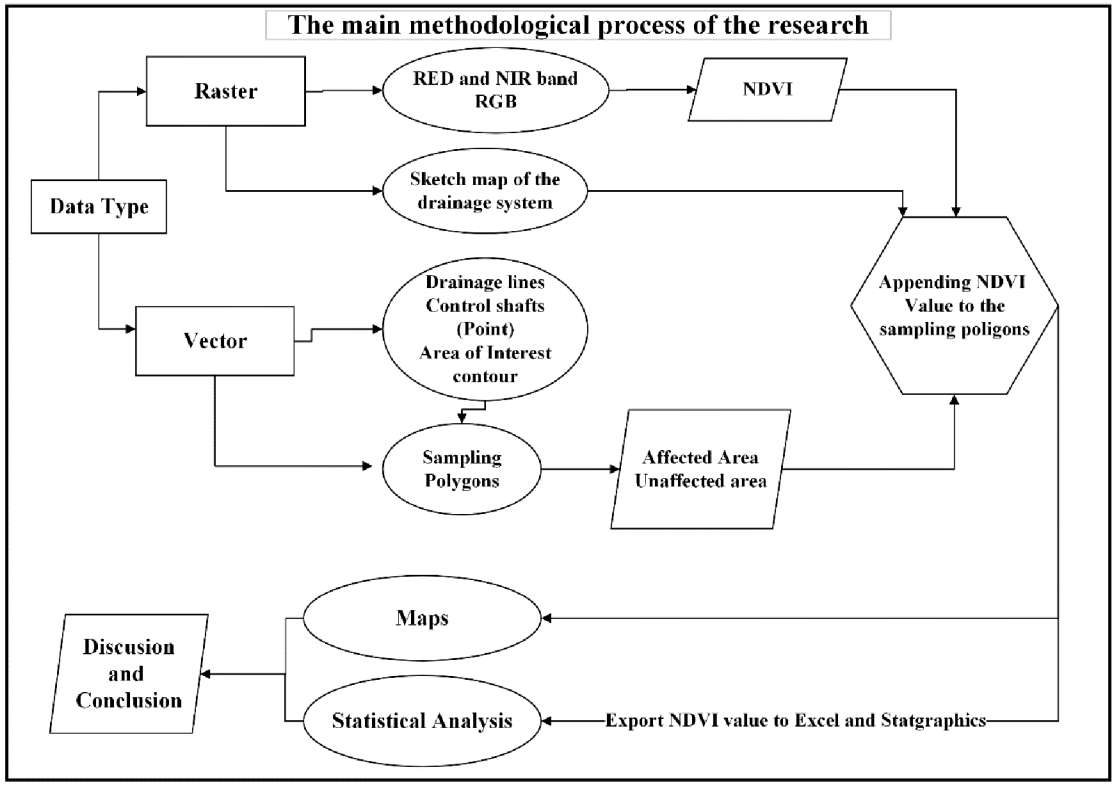

Figure 10: Scheme of the main applied methodological approach of the study

3.3 Source data and sampling polygons

The source satellite images are downloaded from Earth Observation System (EOS). Which is a Land Viewer online platform consisting of satellite imageries with more than seven band combinations. Out of the seven bands the Red and Near infrared bands were downloaded for use in this work to determine the normalized difference vegetation index (NDVI). The Sentinel-2 satellite collects imageries in every second- and third-day of revisiting time at mid latitude area (Hoersch, 2013). On average, the satellite collects twelve imageries per month. However, it is not possible to use all of them. Because of cloud cover and haze. As it is visualized in the Table 1, the cloud cover of scenes is categorized into five parts. Scenes with less than five percent cloud cover is automatically qualified for analysis. On the contrary, scenes with cloud cover more than 21% are omitted from the analysis automatically. Scenes with cloud coverage 6-25% are included in the analysis exceptionally if the cloud cover is out of the study area. The percentage of cloud cover is found from the metadata of the scenes.

To avoid the effect of the soil reflectance on the calculation of NDVI; only the imageries in the time range of the plant growing season is used. This time range is from April to October; seven months

To obtain reliable results, a set of images from years 2019 and 2020 was downloaded. However, because of absence of water level data in the drainage system from 2019, the images downloaded for this year could not be included in the analysis.

Table 1: Colour code of percentage of cloud cover on the downloaded scenes

Parentage of cloud cover	**Color code**
0-5%	
6-10%	
11-25%	
>26%	
No Scene	

Because of the above-mentioned criteria there are some months with zero scene for analysis and there are months up to maximum of six usable scenes in a single month (Table 2). The months with maximum usable scenes are April 2019 and August 2020.

Table 2: The number and usability of the downloaded scenes for years 2019 and 2020

Year	Month	0-5%	6-10%	11-25%	>25%	No. scene	No. of available scenes in the month	No. of usable scenes in the month
2019*	April	6	0	1	6	17	13	7
	May	1	0	0	12	18	13	1
	June	3	1	3	5	18	12	5
	July	2	0	2	9	18	13	3
	August	0	1	1	10	19	12	2
	September	4	0	0	8	18	12	4
	October	0	1	1	10	19	12	1
2020	April	5	0	0	7	18	12	5
	May	2	0	0	10	19	12	1
	June	1	0	0	10	19	11	4
	July	2	0	0	10	19	12	2
	August	6	0	2	2	21	10	2
	September	4	0	0	9	17	13	4
	October	0	0	1	11	19	12	0

** The data from 2019 is not used in the analysis because of non-existence of the record for the water level in the CD system*

In total, 20 sampling polygons are used to append the NDVI value into a vector format within the study area. There are 10 polygons in the affected area and 10 polygons in the unaffected area. The polygons are not equally distributed; higher concentration of sampling polygons is close to the main regulation control shafts (Figure 11). The size of each sampling polygon was 100 m^2. The size exactly corresponds with the pixel size of the calculated NDVI raster file, which is 10-m resolution. The interpolated value of NDVI of each polygon is appended into the attribute as a single value to a centre point of the sampling polygon (Figure 11) for every observation (the available scene of the analysis period).

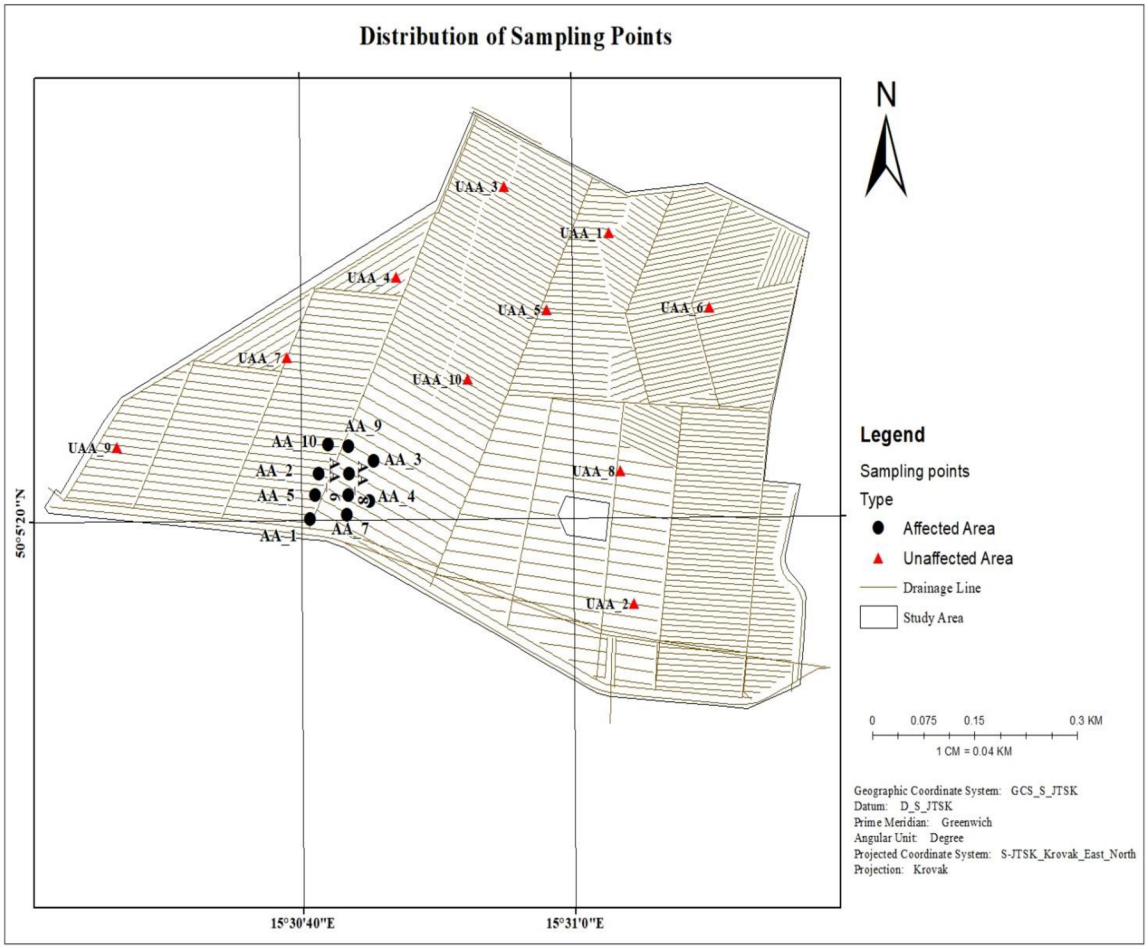

Figure 11: Distribution of the sampling points within the scheme of controlled drainage

Field research has been carried out to determine the exact position of the main regulation shaft in April 2021 (Figure 10)

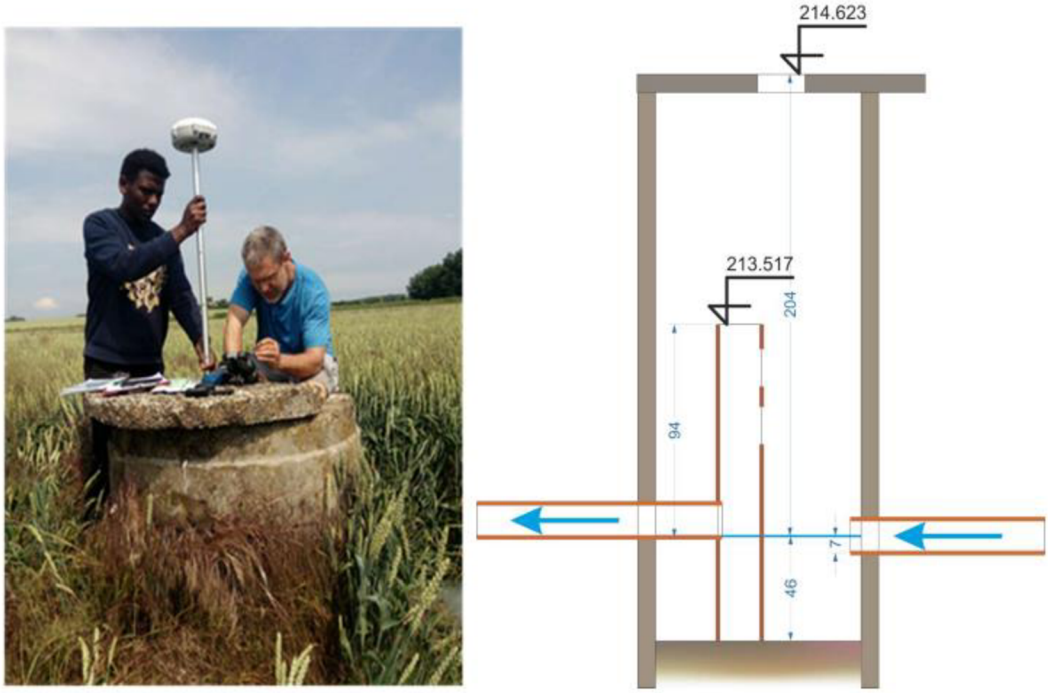

Figure 12: Reading the Exact localization of the control shaft by geodetical GPS. Source: Photo: K. Báťková; Scheme: V. David

3.4 Data processing

The following source data were utilized in this work:

i) The satellite imagery downloaded from the EOS; Level 2-A which means images after Scene Classification and an Atmospheric Correction.

ii) Vector and raster data of the study area (provided by DWR, CULS Prague):
vector data: study area boundary, the drainage pipeline system;
raster data: - plan of the drainage system.

iii) The precipitation and temperature data from The Czech Hydrometeorological Institute (Český hydrometeorologický ústav - ČHMÚ). The data is collected from Radovesnice II meteorological station (Středočeský kraj, (district) Kolín).

3.5 Analysis procedure

3.5.1 ArcGIS operations

To achieve the objective of the study the analysis is made in the following sequence. First, the downloaded scenes were clipped by the area of interest (boundary of the study area). Then the NDVI value for each scene was calculated using raster calculator tool of ArcGIS 10.8. The calculation was made using the NDVI calculation formula (reference to the equation) written into the command line (Figure 13).

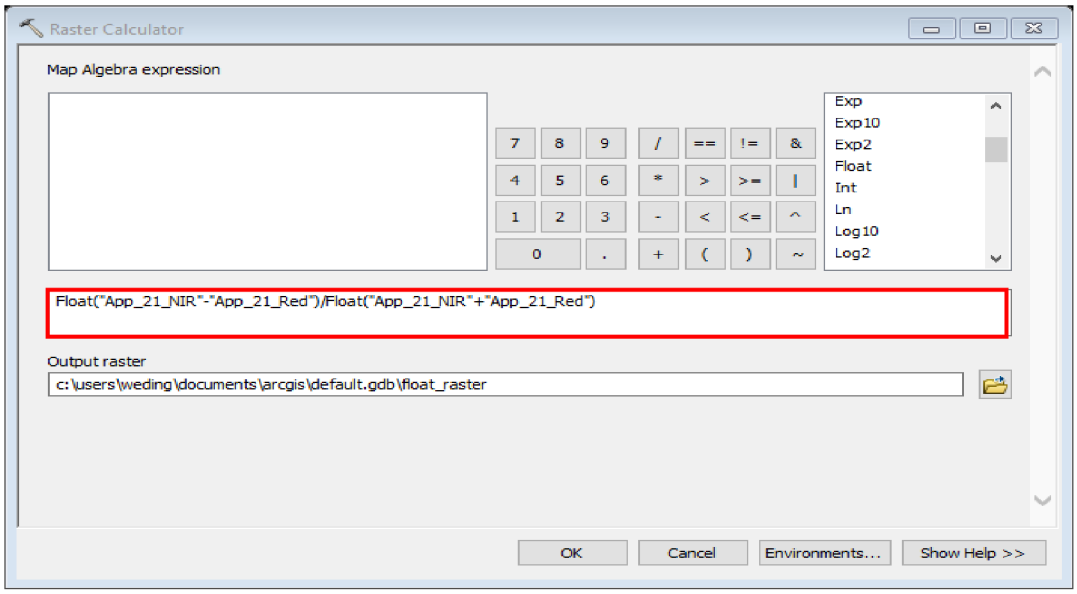

Figure 13: Raster calculator ArcGIS tool with indication of the NDVI calculation (in red rectangle). Source: Arc map 10.8

Transfer of the calculated NDVI values (in a raster form) into the analysable vector format is done by means of the appended attribute of the centre point (sampling point) of each of the sampling polygon. This task was completed using zonal statistics tool of ArcGIS software package. Finally, the attributes of the sampling polygons were exported in the form of editable table (.csv) in MS Excel for further analysis, comparison, and statistical evaluation.

3.5.2 Processing of data exported from ArcGIS

The exported data from Arc GIS software in .csv format were imported into the MS Excel, in which the NDVI values were compared and evaluated.

The resulting NDVI values were evaluated with respect to time for the vegetation season from April 2020 to October 2020. Combination of available NDVI data, with low or no daily precipitation sums, and periods with increased water level within the drainage system indicated by the water level height defined the dates for which the NDVI values of the sampling points (interpolated NDVI for centres of sampling polygons) could be evaluated. Only for these dates, the effect of increased water level in the drainage system can serve as a subsurface irrigation and can help to meet the water requirements of the plants and the differences between the affected and unaffected areas can be observable.

3.6 Statistical evaluation

The analysis of variance (ANOVA) on a significance level $\alpha = 0.05$ has been utilised in order to identify the significance of the differences in the NDVI values determined for CD affected and unaffected areas for the selected dates. Statgraphics Centurion 19 (Statgraphics Technologies, Inc.) has been employed to compare the NDVI values in the multifactor analysis of variance with the following factors: regulation (in operation, out of operation) and area type (CD affected, CD unaffected), interaction between the factors has been also evaluated.

4 Results

4.1 Meteorological conditions and NDVI development in the sampled area

Averaged daily temperatures (°C) together with the daily precipitation sums (mm) were observed (Figure 14). In total, 23 images for the experimental period from April 2020 to October 2020 were analysed (Figure 15) in terms of NDVI. The individual values, together with their averages are displayed on Figure 15. Natural increase of the NDVI of the sunflowers grown in the field was observed from beginning of the vegetation season to its maximum during summer period which was followed by the decrease in the pre-harvesting period. The highest NDVI value (0.84) was observed 1 Aug. 2020 in the area affected by CD, although the water level regulation was out of order and there was no water in the control shaft at that time. The lowest NDVI value (0.15) was recorded 8 May in the area unaffected by CD when the regulation was in operation. The appearance of the experimental field during wet and dry conditions is demonstrated in Figure 16.

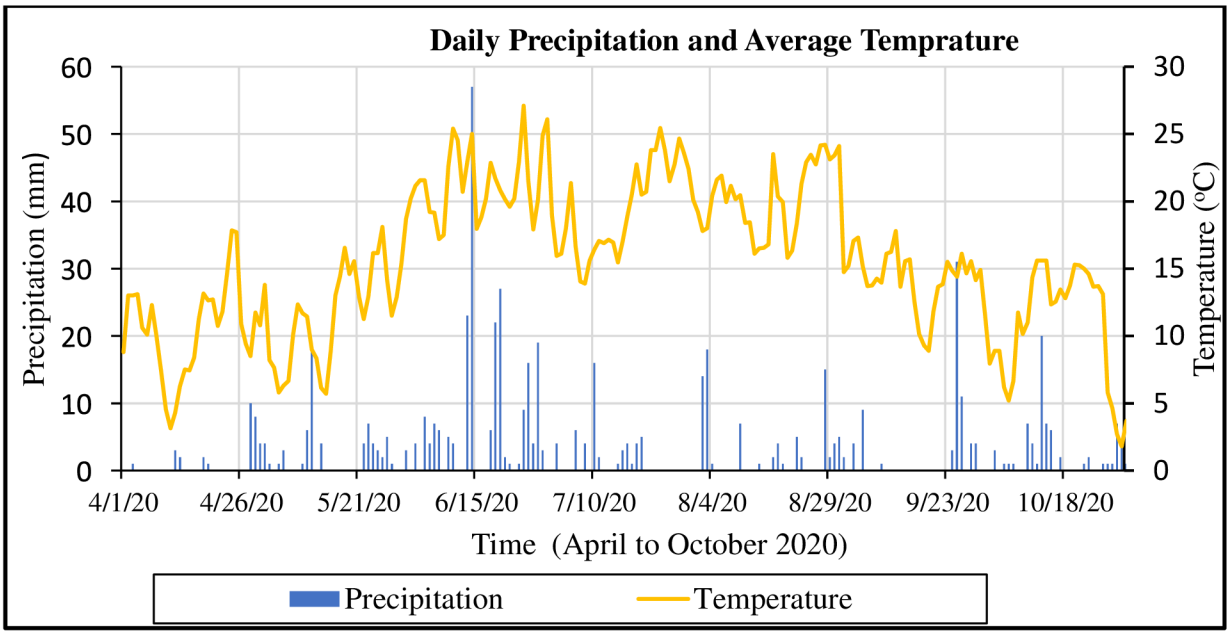

Figure 14: Meteorological data of the study area. Source: The Czech Hydrometeorological Institute (Český hydrometeorologický ústav (ČHMÚ))

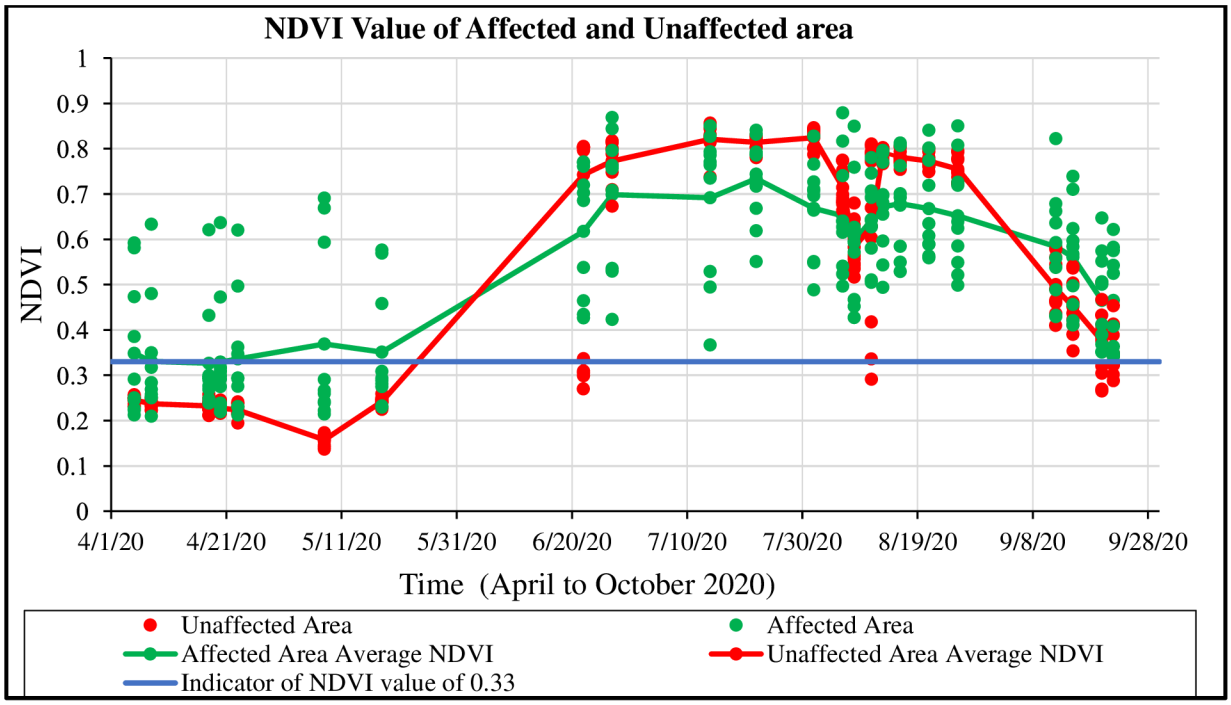

Figure 15: The NDVI values of the sampled area for the year 2020. NDVI calculated values which are above the target line (0.33 NDVI value) are considered as an indicator of healthy plant

Figure 16: Appearance of the experimental field after heavy rains in June 2020 and after dry period in September, when the deep cracks in the soil were present. Source: Kulhavý et al. (2020)

4.2 NDVI in relation to water level and precipitation

Although 23 scenes were downloaded and evaluated, only three could be used for the NDVI comparison and consequent analysis detecting any possible effect of the control drainage system.

It is documented in Figure 18, where precipitation, water levels in the control shaft together with the NDVI values for affected and unaffected areas are plotted. The three dates suitable for the evaluation were: 8 May, 18 May, and 22 June 2020. Clear effect of the CD in operation can be observed for the NDVI determined for the 8 and 18 May, while the third scene (22 June) reflects the situation with sufficient/superfluous amount of water due to rich rain period (Figure 18). The scenes downloaded after 7 July were not used for the NDVI comparison, because the water level in the system was not regulated and water levels in the control shaft were for the rest of the experimental period 0 cm. The hypothesis that higher NDVI value will be reached at the time of higher water level in the drainage system in the period of lower precipitation for area affected by CD has been confirmed. As expected the NDVI value in the unaffected area did not show higher NDVI values since the area is out of reach of the CD. For the sampling time after 7 July 2020, only natural precipitation was affecting the NDVI values on both areas and the NDVI values for the unaffected areas were higher than for the affected area (Figure 17).

Based on the results, the data derived from the scenes downloaded for the selected three dates are sufficient for indication of the effect of the controlled drainage system, as the NDVI values correspond to the easily available water supplied by precipitation or increased level in the control drainage system.

The appearance of the study area displayed in natural resolution (RGB) and in terms of NDVI for the initial, middle, and late stages of sunflower crop is displayed in Figure 17. Growing plants not fully covering the field during the initial stage are on the left, sunflowers during the middle stage are in the middle and late stage just before harvest is on the right.

The appearance of the study area displayed in natural resolution (RGB) and in terms of NDVI for the three evaluated dates is displayed in Figure 18. Growing plants not fully covering the field in May are on the left and in the middle (8 May on the left, 18 May in the middle) and grown sunflowers in June 22 are in the right.

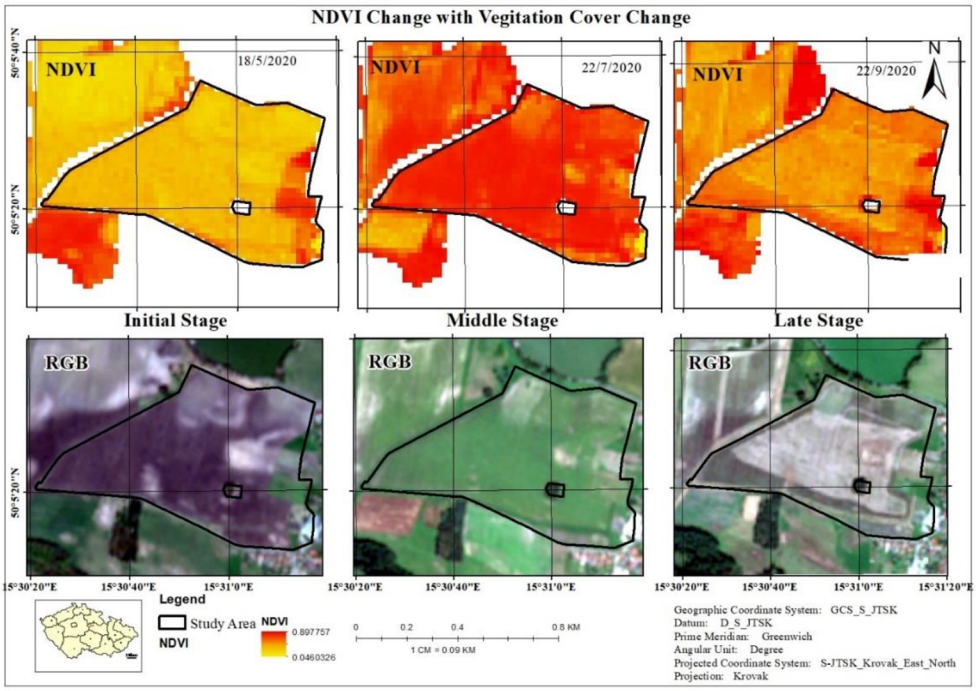

Figure 17: NDVI and RGB change in the three stages of the sunflower. The NDVI and RGB comparison on three development stages of the sunflower

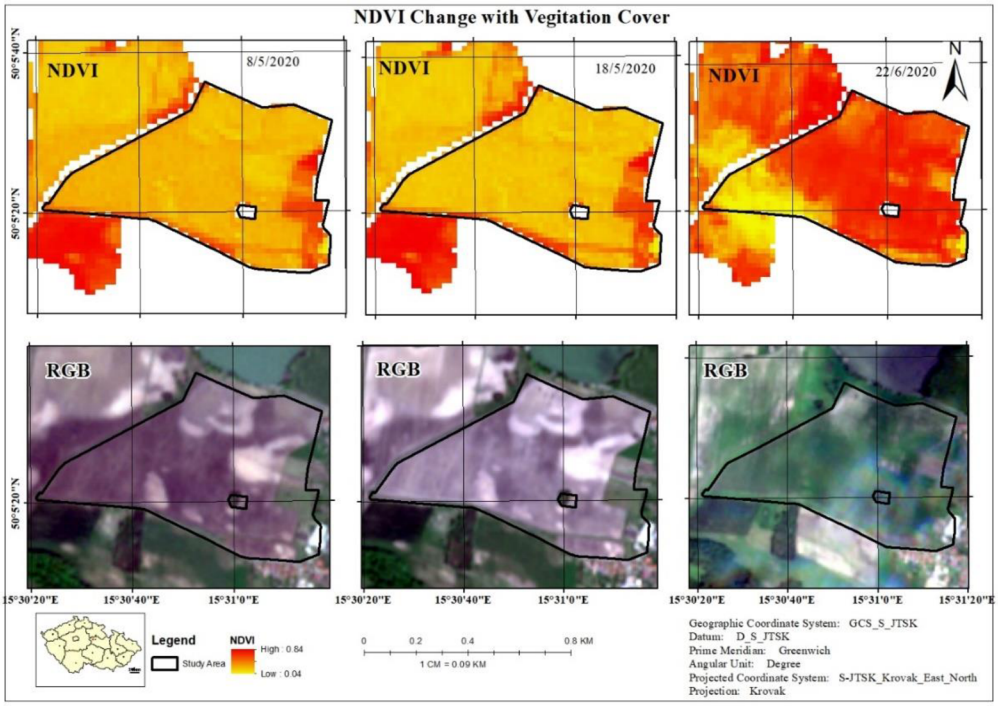

Figure 18: NDVI and RGB map of three chosen days to assess the impact of precipitation and water level; left (8 May), middle (18 May), right (22 June)

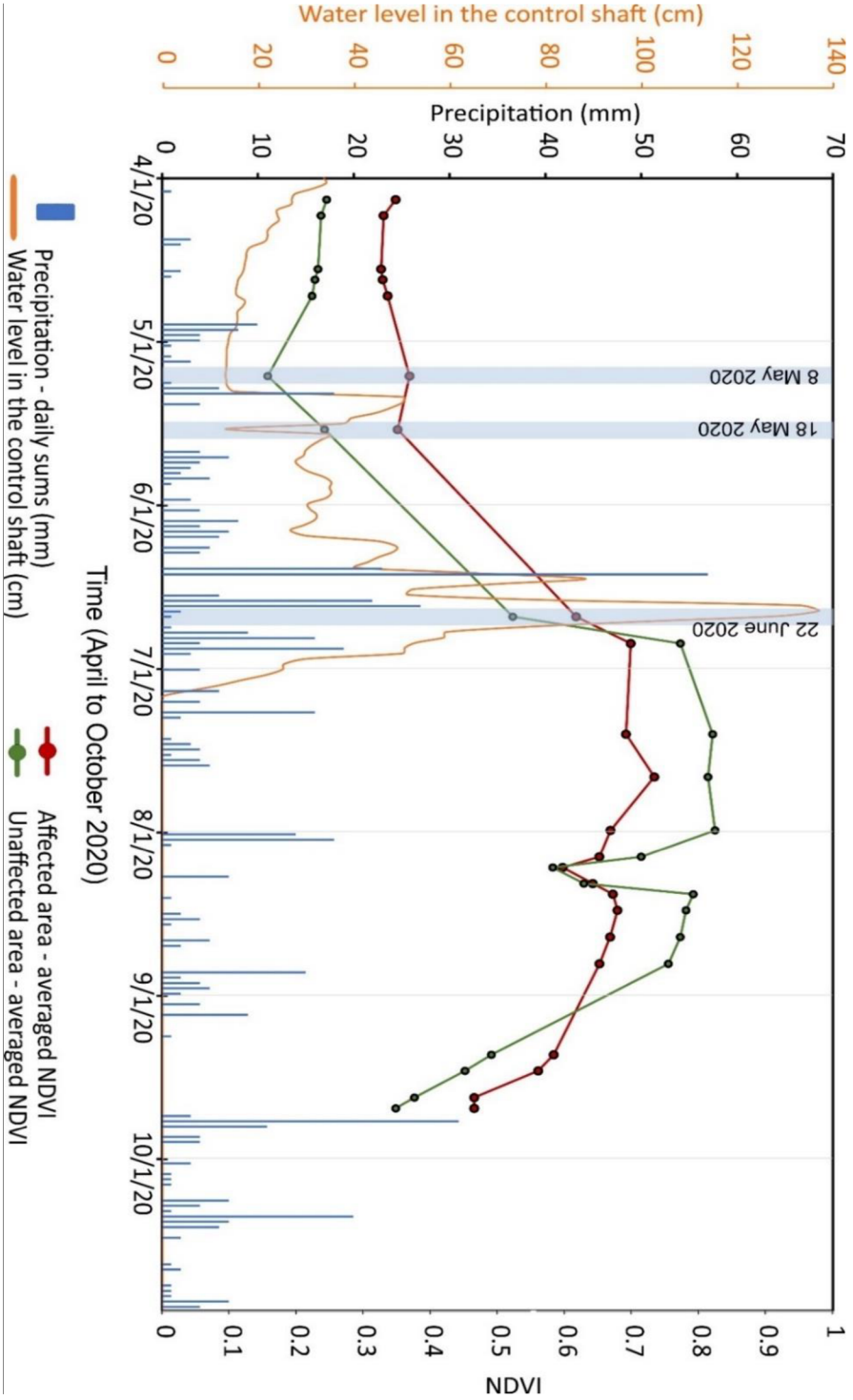

Figure 19: The development of NDVI values in relation to precipitation and water level position in the drainage system; comparison for areas affected and unaffected by CD with indication of the three dates for which the statistical analysis is conducted

4.3 Comparison of NDVI within affected area and unaffected area

The boxplot diagram graphically displays the numerical NDVI data for given sampling dates through their quartiles; the body of the box-plot is from the first to the third quartile, while within the box a vertical line representing the median of the data set and a cross representing the average are located. Outliers (individual points) differ significantly from the rest of the dataset under evaluation.

Figure 20 compares the NDVI values for the selected dates for the areas affected by CD and unaffected by CD. Higher NDVI values were found for affected area in May (on both dates) while in June after the heavy rain, the NDVI values did not differ significantly.

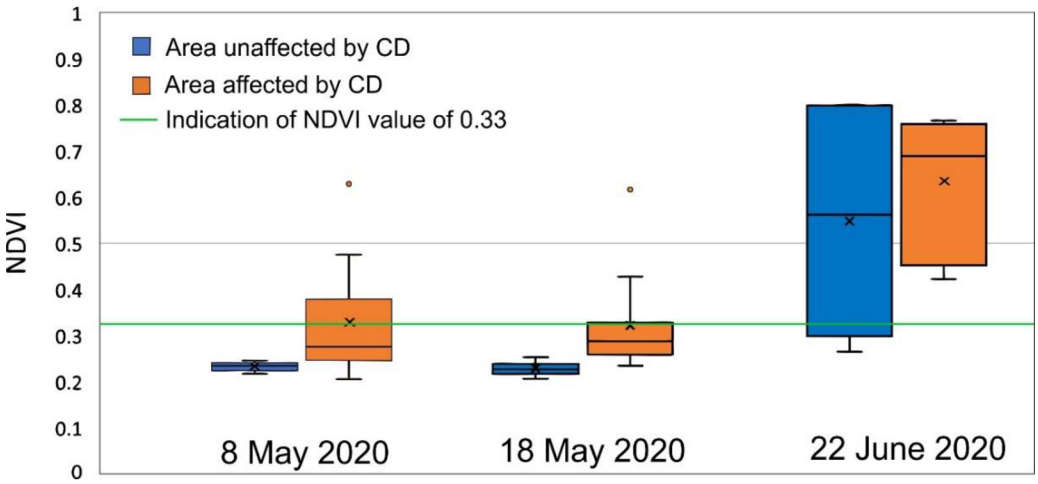

Figure 20: Boxplot comparing the NDVI values for affected and unaffected area by CD

4.4 NDVI comparison with controlled drainage functionality

The analysis of variance (ANOVA) has been applied on the whole dataset of 23 NDVI datasets to evaluate the effect of the control drainage on the NDVI. Generally, the higher (but not statistically significantly higher) values of NDVI were observed for area affected by CD (Figure 21). The graphical comparison showing the interaction of factors: 1) Area type (affected, unaffected) and 2) Regulation (in operation, out of operation) is presented in Figure 22. Statistically significant difference (significance level 0.05) was observed; higher values of NDVI were found for area affected by CD in the period when the regulation was in operation (Figure 22).

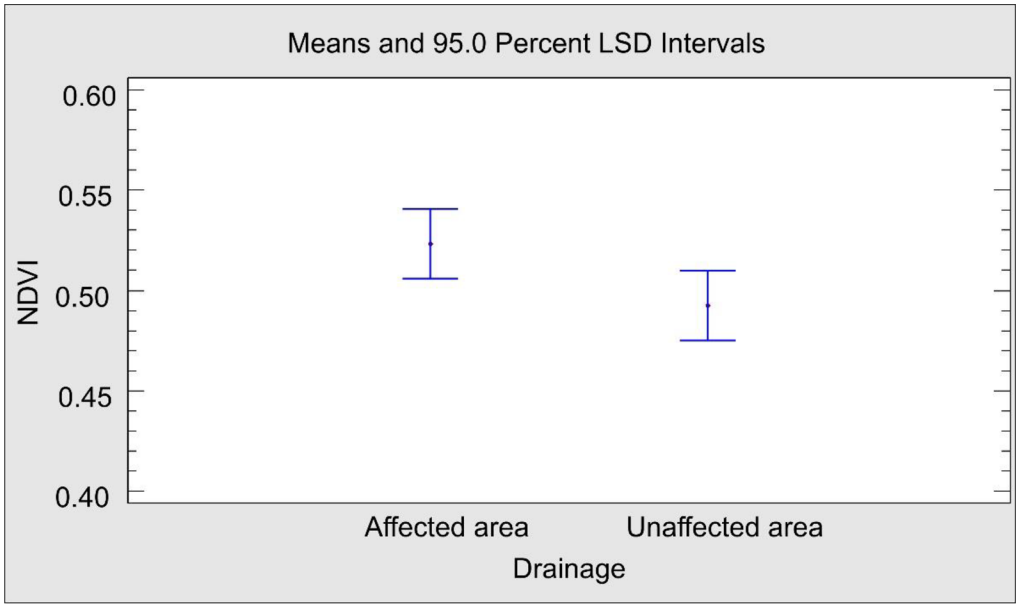

Figure 21: Comparison of NDVI values between drainage affected area and unaffected area for the whole vegetation season without the effect of the regulation status

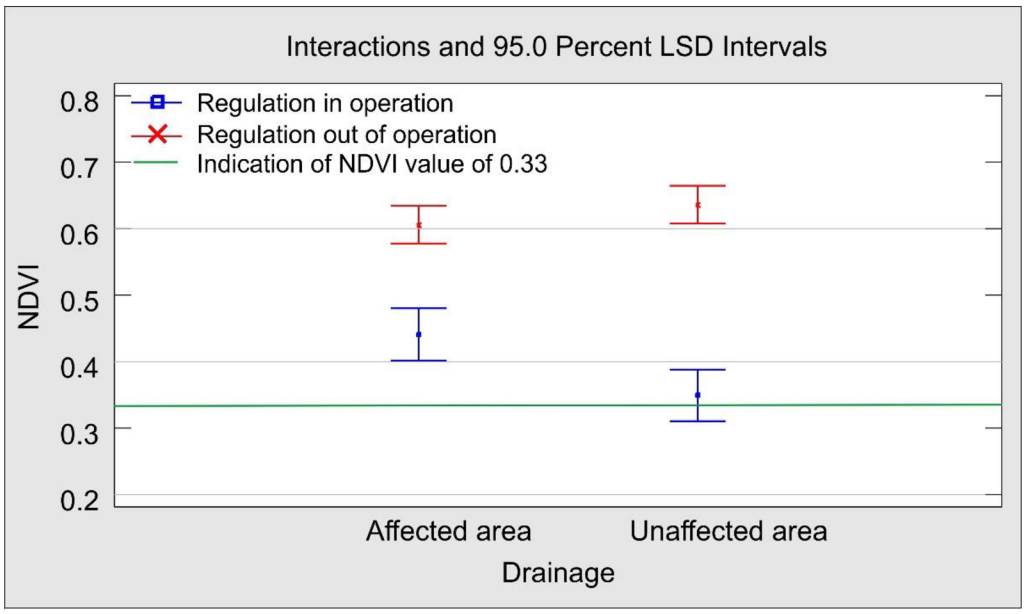

Figure 22: Comparison of NDVI values between drainage affected area and unaffected area in relation to the regulation status (in/out of operation)

5 Discussion

5.1 NDVI value comparison of the sampled area

The NDVI of the study area was calculated separately for the days with available satellite imagery in 2020. As the study area is agricultural land; no NDVI value less than zero indicating the non-vegetation object, was determined in both, CD affected and CD unaffected areas. The highest NDVI value observed in 2020 was 0.88. The value was recorded in August from CD affected area. The lowest NDVI value was recorded on the 8th of May, the observed value was 0.149 reflecting the small plant cover.

The status of the plant growth in the affected area and unaffected area showed a clear difference. Out of the twenty points, ten of the highest variations are recorded from the unaffected area. The NDVI values recorded in the unaffected area in the study period have shown high variation in the plant's health status and stress level. On the opposite side, the CD affected area has shown little variation on the plants NDVI record. This is an indication that the plants in CD affected area were in the better status during the investigated period. The trend of NDVI variation during the study period follows the variation of other factors. These factors are discussed in detail in the following sub sections.

Since the controlled drainage system was in operation only until July 2020, the increase in water level and its effect on the NDVI could be evaluated only for the early time data (April – June). On the other side, the time when the control drainage was out of operation (July – October) can be considered as control when the NDVI values on both areas was not affected by CD.

The found results are in accordance with the conclusion of Bhanja (2019) stating that irrigated crops typically show higher and robust NDVI value than rain fed crops.

5.2 Determining the relationship between NDVI and climate variables

To acquire a reliable NDVI response of the plant, it is important to select the appropriate plant growing season. On this regard, temperature is one major environmental factor which determines the growing season of plants (Barros et al., 2014). Figure 14 showed that the increase in temperature

corresponds with the increase of NDVI value starting from the end of the spring season and the whole summertime. The NDVI and temperature values start declining at the beginning of the autumn.

Temperature is not always facilitating plant growth it can also perform the opposite. This can be explained by the fact that high temperatures lead to higher evaporation, which prohibits growth of the plants which are in the drainage unaffected area (Chuai et al., 2013). Thus, plants from this section are not receiving enough water to replenish water losses due to evapotranspiration.

An interesting point showing a significant NDVI drop was observed at the beginning of August (Figure 19). The trend of temperature value at this period is recorded is higher than the long-term average summer temperature of the area (17.2 ^{o}C). The daily temperature recorded in this period is maximum 26 ^{o}C and minimum 21 ^{o}C. Sunflower is tolerant of both low and high temperatures but less tolerant to high temperature (Putnam and Hicks, 1990). To strengthen this argument, the temperature effect needs to be considered in relation to the precipitation. The precipitation data of the area indicates that there was no precipitation recorded for twelve consecutive days from end of July to the beginning of August. Sunflower has two major characteristics related to water: 1) sunflowers are inefficient water users, and 2) sunflowers are not highly drought tolerant (Putnam and Hicks, 1990). The occurrence of these two characteristics of sunflower and high temperature (higher evapotranspiration) with no precipitation can be the cause for the significant NDVI value drop. Putnam and Hicks (1990) reported sunflowers as very sensitive to water stress during the flowering time, especially in the period 20 days before and 20 days after flowering.

However, the NDVI drop at the beginning of August can be interpreted in another way; that is the flowering stage of the sunflower when the field appears to have yellow colour. The yellow colour of the flowers significantly increased the red band canopy reflectance, but without apparent variations in near infrared. The increase in red band reflectance significantly reduces the NDVI values (Shen et al., 2009). It is probable, that the situation in August 2020 is a result of combination of both above mentioned factors.

5.3 NDVI, water level and precipitation

In the area affected by CD, the lowest ten NDVI values were recorded from the middle of April to the beginning of May, when the soil water level decreased and reached the lowest value of 27.8 cm (Figure 19). In the area unaffected by CD, the lowest ten NDVI values were recorded from the beginning of April up to middle of June, when the precipitation sum was less than 7 mm for more than ten days. The developments a difference in the NDVI values for both, CD affected and CD unaffected areas, in relation to the water level in the drainage regulation shaft together with daily precipitation sums are displayed in Figure 19.

The highest NDVI value in the drainage affected area is obtained on 27th of June (Figure 15) when the soil water level reached the highest level (137 cm). After the period, where the highest precipitation was recorded in the area. This is because the soil has recharged enough amount of water. In another side the highest NDVI value in the drainage unaffected area is recorded in the beginning of July (Figure 15). In this regard the influence of precipitation is very high on both areas.

The NDVI values from the two areas showed differences in spring and also in the summer season, when the difference was relatively higher. Although the regulation was not in the operation, the NDVI value in the drainage affected area for the three summer months showed smaller variation than the values determined for the unaffected area. This can be caused by the selection of the sampling polygons for the CD unaffected area, which covered much larger area and thus soil heterogeneity could provide different conditions for the plants (Figure 19). The majority of NDVI values in the CD unaffected area was higher than in the CD affected area in the summer season. This can be explained by the fact, that sunflowers require good soil drainage (Putnam and Hicks, 1990). Over wetness of the soil causes stress to the plants.

To conclude, difference on plants NDVI response in the two sections of the study area caused by the soil water level regulation and precipitation has been observed. That is why comparison of the NDVI values for selected dates were performed and data was statistically evaluated in order to see the possible significance of the differences.

5.4 Comparison of affected area and unaffected area at three selected dates in 2020

To have an elaborated understanding about the plants status in different stages of the study period in relation to water level in the drainage system and precipitation three dates were selected for detailed evaluation. The following dates, for which all three conditions were fulfilled (scene with low coverage of clouds, increased regulated water level, known – ideally low precipitation), were selected: May 8, May 18 and June 22. The date in June covered completely different conditions than those in April, because there was a lot of precipitation during June and water level in the regulation shaft was reaching its highest level (Figure 19). As a control, a situation after July 7 can be considered, as the water level regulation in the control shaft was not in operation and no water was present and recorded in the system during the rest of the year.

There is a very clear difference between the drainage affected area and unaffected area on 8 and 18 May. Higher NDVI values were found in CD affected area due to the water availability from the drainage system. The NDVI values recorded in the CD affected area showed higher variation probably caused by different distances from the control shaft (Figure 20). The NDVI value recorded on 8 and 18 May in the drainage unaffected area is below the standard NDVI level for healthy plant (> 0.33) (Liu et al., 2019). The NDVI values recorded for the CD unaffected area were consistently lower during the spring period when the CD in the area of affection was supplying water via the system. In the CD affected area, more than 50 % of the recorded NDVI value was higher than the standard healthy plant NDVI level (> 0.33). The NDVI variations in May can also be explained by fact that the plants are at their initial stage of growth and the field is not covered by the plant fully (Richard, 2006).

The third selected day (22/6/2020) shows a higher NDVI value for both areas because the sunflowers are already grown. More interestingly, a significant effect of sufficient precipitation abolished the effect of CD and higher NDVI values were observed in CD unaffected area. But the NDVI value in the unaffected area shows higher variation.

5.5 NDVI comparison with controlled drainage functionality

The impact of the drainage system was not expected to be observed after the 7 July since the regulation shaft was not regulating water in the drainage system. The period the regulation shaft was in operation the difference between the two area was very high. But during the period when the regulation shaft was out of operation, the difference between the CD affected and unaffected areas was very small (Figure 20 and Figure 22) When the regulation shaft was in operation the impact of the regulation system was very high because the precipitation sums were relatively low and plants need more water at the late early and middle growth stage (Herbei and Sala, 2015).

The suitability of the satellite images and NDVI analysis for identification of the effect of CD on the agricultural field has been proved.

6 Conclusion

At the present time the influence of technology in our daily life and decision making ability is growing. One of the areas that shows high level of technological dependability for a better efficiency and productivity is agriculture and natural resources management. Some technologies save time, some save energy, some facilitate accessibility etc. Remote sensing technology helps to assess, monitor and make decisions without a need to go physically to the site. The NDVI calculation technique is one of the products of such a technology.

The NDVI technique is used in the thesis to assess functionality of controlled drainage system in the selected study area (Strašov). From the conducted analysis and obtained results, it is possible to formulate the following conclusions.

- The proposed hypothesis stating, that using the NDVI techniques it is possible to determine the function and/or malfunction of the controlled drainage system has been proved.
- The ANOVA result has shown that the impact of the increased water level within the area affected by controlled drainage has a significant effect on the NDVI.
- Some differences were observed between the NDVI values determined for the area affected and unaffected by controlled drainage in the period when the regulation was set out of operation and the NDVI solely depended on precipitation. These differences can be attributed to the different sizes of the areas. The area affected by controlled drainage was quite small and in a close vicinity from the regulation shaft, while the unaffected area was represented by much larger and possibly more heterogeneous part of the field.
- Most of the studies previously done are large scale in terms of area coverage. The result of this study has proved that this technique can be applied in a smaller scale.
- For the future work, it is advisable to examine the possible reach of the controlled drainage via NDVI comparison of sets of sampling polygons surrounding the control shaft in regular distances. However, this study might require images of higher resolution, which come at cost.

7 References

1. Aggarwal, S. (2005). Satellite remote sensing and GIS applications in agricultural meteorology, Principles of remote sensing. 16.
2. Asrar, G., Fuchs, M., Kanemasu, E., and Hatfield, J. (1984). Estimating absorbed photosynthetic radiation and leaf area index from spectral reflectance in wheat1. Agronomy Journal AGRON J, 76. DOI. 10.2134/000219620076000200 29x
3. Barros, V. R., Field, C. B., Dokken, D. J., Mastrandrea, M. D., Mach, K. J., Bilir, T. E., Chatterjee, M., Ebi, K. L., Estrada, Y. O., Genova, R. C., Girma, B., Kissel, E. S., Levy, A. N., MacCracken, S., Mastrandrea, P. R., and White, L. L. (2014). Climate change 2014 impacts, adaptation, and vulnerability, Cambridge University Press. DOI. 10.1017/ CBO9781107415386
4. Bhanja, S. N., Malakar, P., Mukherjee, A., Rodell, M., Mitra, P., and Sarkar, S. (2019). Using satellite-based vegetation cover as indicator of groundwater storage in natural vegetation areas. Geophysical research letters, 46(14), 8082–8092. DOI. 10.1029/ 2019GL083015
5. Borrelli, P., Alewell, C., Alvarez, P., Anache, J. A. A., Baartman, J., Ballabio, C., Bezak, N., Biddoccu, M., Cerdà, A., Chalise, D., Chen, S., Chen, W., De Girolamo, A. M., Gessesse, G. D., Deumlich, D., Diodato, N., Efthimiou, N., Erpul, G., Fiener, P., Panagos, P. (2021). Soil erosion modelling: A global review and statistical analysis. Science of the total environment, 780, 146494. DOI. 10.1016/j.scitotenv.2021.146494
6. Brázdil, R., Chromá, K., Dobrovolný, P., and Tolasz, R. (2009). Climate fluctuations in the Czech Republic during the period 1961–2005. International Journal of Climatology, 29(2), 223–242. DOI. 10.1002/joc.1718
7. Campbell, J. (1987). Introduction to remote sensing, Fifth Edition. The Guilford press. New York, USA. 667
8. Chuai, X. W., Huang, X. J., Wang, W. J., and Bao, G. (2013). NDVI, temperature and precipitation changes and their relationships with different vegetation types during 1998-2007 in inner Mongolia. International Journal of Climatology, 33(7), 1696–1706. DOI. 10.1002/joc.3543
9. Copernicus. (2021). Copernicus. Europe's eyes on Earth. Europe's Eyes on Earth. https://www.copernicus.eu/en

10. Corinne, W. (2018). Controlled Drainage. Find tools for sustainable sanitation and water management: Sustainable Sanitation and Water Management Toolbox. http://bitly.ws/q6ib, Accessed on: 2022-03-21 11:41
11. Devitt, D., Bird, B., Lyles, B., Fenstermaker, L., Jasoni, R., Strachan, S., Arnone lll, J., Biondi, F., Mensing, S., and Saito, L. (2018). Assessing near surface hydrologic processes and plant response over a 1600 m mountain valley gradient in the great basin of NV, U.S.A. Water, 10(4), 420. DOI. 10.3390/w10040420
12. Dragotti, P. L., & Gastpar, M. (2009). Distributed source coding: Theory, algorithms, and applications. Elsevier inc. 338.
13. Feldman, D. L. (2013). Adaptation as a water resource policy challenge institutions and science. Journal of Water Resource and Protection, 05(04), 1–6. DOI. 10.4236/ jwarp.2013.54A001
14. García-Haro, F. J., Gilabert, M. A., and Meliá, J. (2007). Linear spectral mixture modelling to estimate vegetation amount from optical spectral data. International Journal of Remote Sensing. DOI. 10.1080/01431169608949157
15. Gitelson, A. A. (2004). Wide dynamic range vegetation index for remote quantification of biophysical characteristics of vegetation. Journal of Plant Physiology, 161(2), 165–173. DOI. 10.1078/0176-1617-01176
16. Gitelson, A. A., Gritz †, Y., and Merzlyak, M. N. (2003). Relationships between leaf chlorophyll content and spectral reflectance and algorithms for non-destructive chlorophyll assessment in higher plant leaves. Journal of Plant Physiology, 160(3), 271–282. DOI. 10.1078/0176-1617-00887
17. Gitelson, A. A., Stark, R., Grits, U., Rundquist, D., Kaufman, Y., and Derry, D. (2002). Vegetation and soil lines in visible spectral space: A concept and technique for remote estimation of vegetation fraction. International Journal of Remote Sensing, 23(13), 2537–2562. DOI. 10.1080/01431160110107806
18. Hamed, H. M. (2005). Hyperspectral crop reflectance data for characterising and estimating fungal disease severity in wheat. Elsevier Ltd, 12. DOI. 10.1016/2005.02.007
19. Hasić, S., and Matula, D. S. (2020). Conversion of classical systematic drainage into regulation drainage. Czech University of Life Sciences, Prague, CZ.

20. Henebry, G. M. (2004). The wide dynamic range vegetation index and its potential utility for gap analysis. United States Department of the Interior and the United States Geological Survey, 12, 9.
21. Herbei, M. V., and Sala, F. (2015). Use landsat image to evaluate vegetation stage in sunflower crops. AgroLife Scientific Journal, 4(1). DOI. 2286-0126; ISSN-L 2285-5718
22. Hoersch, B. (2013). ESA standard document: Sentinel-2 user handbook. ESA. https://sentinel.esa.int/documents/247904/685211/Sentinel-2_User_Handbook
23. Huete, A., Didan, K., Miura, T., Rodriguez, E. P., Gao, X., and Ferreira, L. G. (2002). Overview of the radiometric and biophysical performance of the MODIS vegetation indices. Remote Sensing of Environment, 83(1–2), 195–213. DOI.10.1016/S0034-4257(02)00096-2
24. Janssen, L. L. F., Bakker, W. H., (2001). Principles of remote sensing: An introductory textbook. International Institute for Aerospace Survey and Earth Sciences. ITC Educational Textbook Series, 2. ITC. Enschede
25. Kaufman, Y. J., and Tanre, D. (1992). Atmospherically resistant vegetation index (ARVI) for EOS-MODIS. IEEE Transactions on Geoscience and remote sensing, 30(2), 261–270. DOI. 10.1109/36.134076
26. Krusinger, A. E. (1971). Location of drainage tile using aerial photography. Ohio State University. Columbus, Ohio, United States.
27. Kulhavý, Z., and Fučík, P. (2015). Adaptation options for land drainage systems towards sustainable agriculture and the environment: A Czech perspective. Polish Journal of Environmental Studies, 24, 1085–1102. DOI. 10.15244/pjoes/34963
28. Kulhavý, Z., Jakoubek, J., Matula, S., Šťastná, M. (2020). Redakčně upravená roční zpráva výzkumného projektu. QK1910086, 183 pp
29. Liu, Y., Youssef, M. A., Chescheir, G. M., Appelboom, T. W., Poole, C. A., Arellano, C., and Skaggs, R. W. (2019). Effect of controlled drainage on nitrogen fate and transport for a subsurface drained grass field receiving liquid swine lagoon effluent. Agricultural Water Management, 217, 440–451. DOI. 10.1016/j.agwat.2019.02.018
30. Madramootoo, C. A., Johnston, W. R., Ayars, J. E., Evans, R. O., and Fausey, N. R. (2007). Agricultural drainage management, quality and disposal issues in North America. Journal of Irrigation and Drainage Engineering, 124(2), 122-166. DOI. 10.1002/ird.343

31. Motohka, T., Nasahara, K. N., Oguma, H., and Tsuchida, S. (2010). Applicability of Green-Red vegetation index for remote sensing of vegetation phenology. Journal of Remote Sensing, 2(10), 2369–2387. DOI. 10.3390/rs2102369
32. Nováková, E., Karous, M., Zajíček, A. and Karousová, M. (2013). Evaluation of ground penetrating radar and vertical electrical sounding methods to determine soil horizons and bedrock at the locality Dehtáře. Soil and Water Research 8(3), pp 105–112.
33. Oosterbaan, R. J., and Nijland, H. (1994). Determining the saturated hydraulic conductivity. Drainage Principles and Applications.
34. Pettorelli, N., Vik, J. O., Mysterud, A., Gaillard, J.-M., Tucker, C. J., and Stenseth, N. Chr. (2005). Using the satellite-derived NDVI to assess ecological responses to environmental change. Trends in ecology and evolution, 20(9), 503–510. DOI. 10.1016/j.tree.2005.05.011
35. Putnam, D. H., and Hicks, D. R. (1990, November). Alternative field crop manual: Sunflower. Departments of agronomy and plant genetics, Entomology and plant pathology, University of Minnesota]. https://www.hort.purdue.edu/newcrop/afcm/sunflower
36. Qi, J., Chehbouni, A., Huete, A. R., Kerr, Y. H., and Sorooshian, S. (1994). A modified soil adjusted vegetation index. Journal of Remote Sensing of Environment, 48(2), 119–126. DOI. 10.1016/0034-4257(94)90134-1
37. Reddy, M.A. (2008). Textbook of remote sensing and geographical information systems (Third Edition). BS Publications. 476.
38. Richard, G. A. (2006). FAO irrigation and drainage paper No 56. Food and Agriculture Organization (FAO) UN. https://academic.uprm.edu/abe/backup2/tomas/fao%2056.pdf
39. Richardson, A. J. (1978). Distinguishing vegetation from soil background information. Japan Society of Photogrammetry, 43(12).
40. Ritzema, H. (2007). Performance Assessment of Subsurface Drainage Systems Case Studies from Egypt and Pakistan. Alterra-ILRI Wageningen University and Research Centre Wageningen, 138.
41. Roberts, F. S. (1984). Measurement theory with applications to decision making, utility, and the social sciences. Cambridge University Press.
42. Rondeaux, G., Steven, M., and Baret, F. (1996). Optimization of soil-adjusted vegetation indices. Remote Sensing of Environment, 55(2), 95–107. DOI. 10.1016/0034-4257(95)00186-7

43. Rouse Jr, J. W., Haas, R. H., Deering, D. W., and Schell, J. A. (1973). Monitoring the vernal advancement and retrogradation (Green Wave Effect) of natural vegetation. Texas university remote sensing canters college station, Texas.
44. Samapriya, R. (2013). Remote sensing and gis applications for drainage detection and modelling in agricultural watersheds. Indiana University.
45. Schowengerdt, R. A. (2007). Remote sensing: models, and methods for image processing (3rd ed). Academic Press. Waltham, 2.
46. Shao, G., Cui, J., Yu, S., Lu, B., Brian, B. J., Ding, J., and She, D. (2015). Impacts of controlled irrigation and drainage on the yield and physiological attributes of rice. Agricultural water management, 149(C), 156–165.
47. Shedekar, V., Brown, L., Delgado, J., Sassenrath, G., and Mueller, T. (2017). GIS and GPS Applications for planning, design and management of drainage systems. DOI. 0.2134/ agronmonogr59.2013.0026
48. Shen, M., Chen, J., Zhu, X., and Tang, Y. (2009). Yellow flowers can decrease NDVI and EVI values: Evidence from a field experiment in an alpine meadow. Canadian Journal of Remote Sensing, 35, 99–106. DOI. 10.5589/m09-003
49. Sneha, C., Santhoshkumar, A. V., and Sunil, K. M. (2012). Effect of controlled irrigation on physiological and biometric characteristics in teak (Tectona grandis) seedlings. 8(3), 8.
50. Tlapáková, L. (2017). Development of drainage system in the Czech landscape – identification and functionality assessment by means of remote sensing. European Countryside, 9(1), 77–98. DOI. 10.1515/euco-2017-0005
51. USDA. (1974). Chapter 1: Principles of drainage. United States Department of Agriculture, Washington, DC., 16, 34.
52. USDA. (2001). Part 650 engineering field handbook national engineering handbook: Water management (drainage). USDA, Washington, DC.
53. Viña, A., Henebry, G. M., and Gitelson, A. A. (2004). Satellite monitoring of vegetation dynamics: Sensitivity enhancement by the wide dynamic range vegetation index. Geophysical Research Letters, 31(4). DOI. 10.1029/2003GL019034
54. Xue, J., and Su, B. (2017). Significant remote sensing vegetation indices: A Review of developments and applications. journal of sensors, 2017, 1–17. DOI. 10.1155/ 2017/1353691

55. Yadav, S. K., Raj, S., and Roy, S. S. (2013). Remote sensing technology and its applications. International Journal of Advancement in Research and Technology, 2(10), 6.

8 List of Figures

9 List of Tables

10 List of Equations

Eq 1 $RVI = R/NIR$

Eq 2 $DVI = NIR - R$

Eq 3 $PVI = \sqrt{(\rho soil - \rho veg)2\ R - (\rho soil - \rho veg)2NIR}$

Eq 5 $NDVI = \frac{(NIR-Red)}{(NIR+Red)}$

Eq 6 $WDRVI = \frac{(\alpha*NIR-Red)}{(\alpha*NIR+Red)}$

Eq 7 $ARVI = \frac{(NIR-RB)}{(NIR+RB)}$

Eq 8 $VARI = \frac{(Green-Red)}{(NGreen+Red-Blue)}$

Eq 9 $EVI = 2.5 * \frac{(NIR-Red)}{((NIR)+(C1*Red)-(C2*Blue)+L)}$

Eq 10 $EVI = 2.5 * \frac{(NIR-Red)}{(NIR+6*RED-7.5*Blue+1)}$

Eq 11 $SAVI = \frac{(NIR-Red)}{(NIR+RED+L)} * (1+L)$

Eq 12 $SAVI = \frac{1.5*(NIR-Red)}{(NIR+RED+0.5)}$

Eq 13 $MSAVI2 = \frac{2*NIR+1-\sqrt{(2*NIR+1)^2-8(NIR-Red}}{2}$

Eq 14 $OSAVI = \frac{(NIR-Red)}{(NIR+RED+0.16)}$

Eq 15 $GCI = \frac{(NIR)}{(Green)} - 1$

Eq 16 $SIPI = \frac{NIR-Blue}{NIR-Red}$

11 List of Symbols and Acronyms

α = alpha, weighting coefficient, ranges from 0.1 to 0.2

C1=values as coefficients for atmospheric resistance

C2 =values as coefficients for atmospheric resistance

L= Value to adjust for canopy background

AVHRR - Advanced Very-High-Resolution Radiometer

ADS - Agricultural drainage systems

ANOVA – Analysis of Variance

ARVI - Atmospherically resistant vegetation index

CTD - Controlled tile drainage

CR - Czech Republic

DVI - Difference Vegetation Index

EOS – Earth-observing system

EM - Electromagnetic

ETM+ - Enhanced Thematic Mapper Plus

EVI - Enhanced vegetation index

ESA - European Space Agency

ET - Evapotranspiration

GIS - Geographic Information System

GOES - Geostationary Operational Environmental Satellite

GEMI - Global Environmental Monitoring Index

GPS - Global Positioning system

GCI - Green Chlorophyll Index

LAI - Leaf Area Index

LSD – Least Significant Difference

LIDAR - Light Detection and Ranging

LPIS - Land Parcel Identification System

MODIS - Moderate Resolution Imaging Spectroradiometer

MSAVI - Modified soil adjusted vegetation index

NASA - National Aeronautics and Space Administration

NM - Nanometres

NIR - Near Infrared

NDVI - Normalized Difference Vegetation Index

OSAVI - Optimized Soil Adjusted Vegetation Index

PVI - Perpendicular Vegetation Index

PVC - Polyvinyl chloride

PLC - Programmable logic controller

RVI - Ratio Vegetation Index

RS - Remote sensing

SAVI - Soil Adjusted Vegetation Index

SIPI - Structure Insensitive Pigment Index

TM - Thematic Mapper

TSAVI - Transformed Soil-Adjusted Vegetation Index

UCTD - Uncontrolled tile drainage

USGS - United States Geological Survey

VF - Vegetation fraction

VI - Vegetation index

VARI - Visible Atmospherically Resistant Index

WDRVI - Wide Dynamic Range Vegetation Index

Appendix 1 - Calander of the downloaded scenes

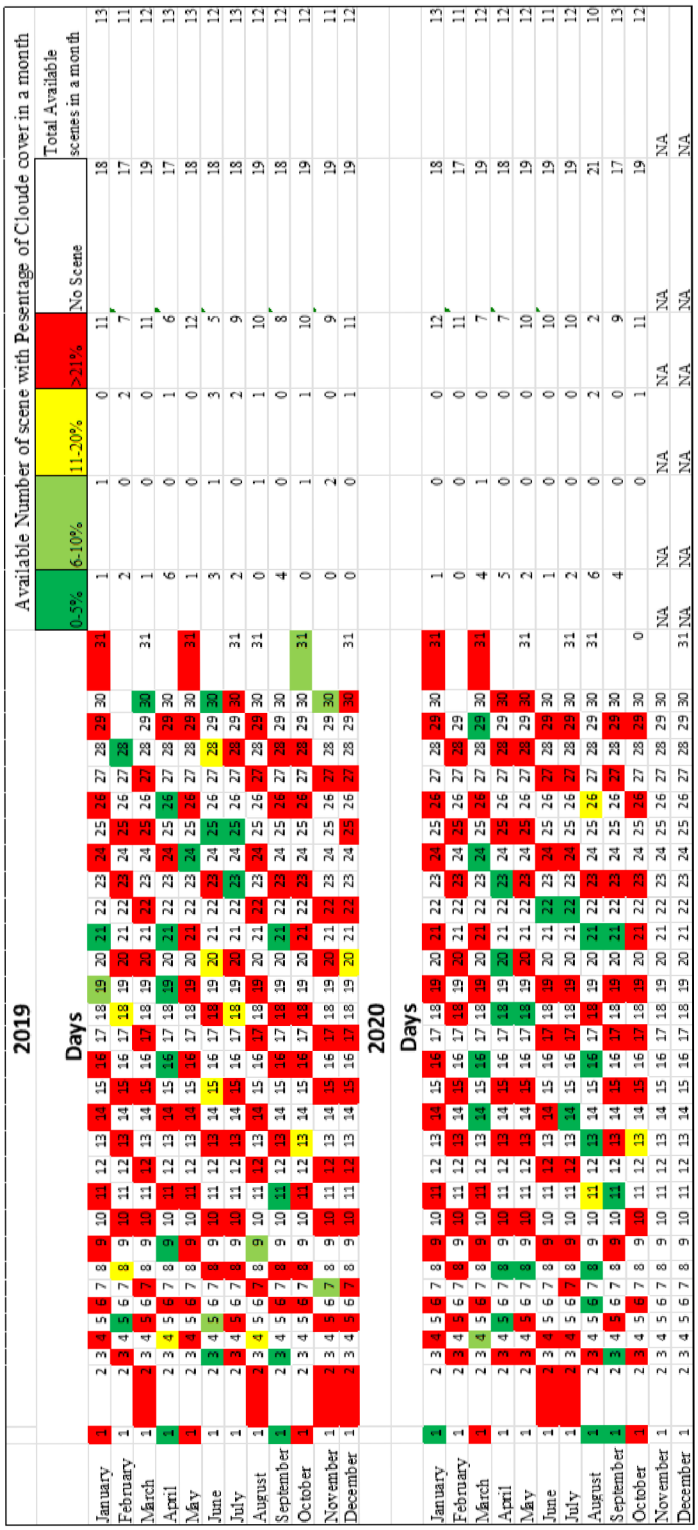

Appendix 2 – Statistical evaluation in Statgraphics

Multifactor ANOVA - NDVI

General Linear Models

Number of dependent variables: 1
Number of categorical factors: 2
A=Drainage – affected/unaffected area
B=Regulation – in operation/out of operation
Number of quantitative factors: 0

Analysis of Variance for NDVI

Source	*Sum of Squares*	*Df*	*Mean Square*	*F-Ratio*	*P-Value*
Model	8.52288	3	2.84096	90.52	0.0000
Residual	14.311	456	0.0313838		
Total (Corr.)	22.8339	459			

Type III Sums of Squares

Source	*Sum of Squares*	*Df*	*Mean Square*	*F-Ratio*	*P-Value*
Drainage	0.103766	1	0.103766	3.31	0.0697
Regulation	8.08225	1	8.08225	257.53	0.0000
Drainage*Regulation	0.405192	1	0.405192	12.91	0.0004
Residual	14.311	456	0.0313838		
Total (corrected)	22.8339	459			

Expected Mean Squares

Source	*EMS*
Drainage	(4)+Q1
Regulation	(4)+Q2
Drainage*Regulation	(4)+Q3
Residual	(4)

F-Test Denominators

Source	*Df*	*Mean Square*	*Denominator*
Drainage	456.00	0.0313838	(4)
Regulation	456.00	0.0313838	(4)
Drainage*Regulation	456.00	0.0313838	(4)

Variance Components

Source	*Estimate*
Residual	0.0313838

R-Squared = 37.3256 percent
R-Squared (adjusted for d.f.) = 36.9132 percent
Standard Error of Est. = 0.177155
Mean absolute error = 0.145575
Durbin-Watson statistic = 0.674578 (P=0.0000)

Residual Analysis

	Estimation	*Validation*
n	460	
MSE	0.0313838	
MAE	0.145575	
MAPE	33.6185	
ME	-2.84796E-16	
MPE	-14.438	

The StatAdvisor
This pane summarizes the results of fitting a general linear statistical model relating NDVI to 2 predictive factors. Since the P-value in the first ANOVA table for NDVI is less than 0.05, there is a statistically significant relationship between NDVI and the predictor variables at the 95.0% confidence level.

The second ANOVA table for NDVI tests the statistical significance of each of the factors as it was entered into the model. Notice that the highest P-value is 0.0697, belonging to A. Since the P-value is greater or equal to 0.05, that term is not statistically significant at the 95.0% confidence level. Consequently, you should consider removing A from the model. The R-Squared statistic indicates that the model as fitted explains 37.3256% of the variability in NDVI. The adjusted R-squared statistic, which is more suitable for comparing models with different numbers of independent variables, is 36.9132%. The standard error of the estimate shows the standard deviation of the residuals to be 0.177155. This value can be used to construct prediction limits for new observations by selecting the Reports option from the text menu. The mean absolute error (MAE) of 0.145575 is the average value of the residuals. The Durbin-Watson (DW) statistic tests the residuals to determine if there is any significant correlation based on the order in which they occur in your data file. Since the P-value is less than 0.05, there is an indication of possible serial correlation. Plot the residuals versus row order to see if there is any pattern that can be seen.

The output also summarizes the performance of the model in fitting the data, and in predicting any values withheld from the fitting process.
It displays:
(1) the mean squared error (MSE)
(2) the mean absolute error (MAE)
(3) the mean absolute percentage error (MAPE)
(4) the mean error (ME)
(5) the mean percentage error (MPE)
Each of the statistics is based on the residuals. The first three statistics measure the magnitude of the errors. A better model will give a smaller value. The last two statistics measure bias. A better model will give a value close to 0.

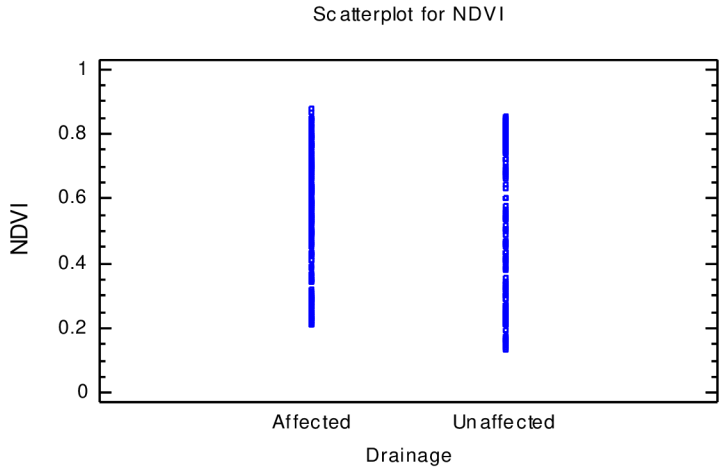

95.0% confidence intervals for coefficient estimates (NDVI)

		Standard			
Parameter	*Estimate*	*Error*	*Lower Limit*	*Upper Limit*	*V.I.F.*
CONSTANT	0.502858	0.00846226	0.486229	0.519488	
Drainage	0.0153873	0.00846226	-0.00124265	0.0320171	1.0496
Regulation	-0.1358	0.00846226	-0.15243	-0.11917	1.0
Drainage*Regulation	0.0304063	0.00846226	0.0137764	0.0470362	1.0496

The StatAdvisor
This table shows 95.0% confidence intervals for the coefficients in the model.

Confidence intervals show how precisely the coefficients can be estimated given the amount of available data and the noise which is present. Also included are variance inflation factors, which can be used to measure the extent to which the predictor variables

are correlated amongst themselves. VIF's above 10, of which there are 0, are usually considered to indicate serious multicollinearity. Serious multicollinearity greatly increases the estimation error of the model coefficients as compared with an orthogonal sample.

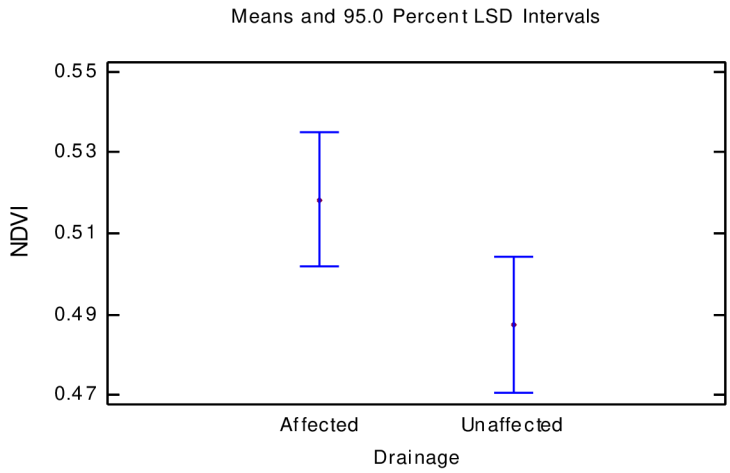

Table of Least Squares Means for NDVI
with 95.0 Percent Confidence Intervals

			Stnd.	*Lower*	*Upper*
Level	*Count*	*Mean*	*Error*	*Limit*	*Limit*
GRAND MEAN	460	0.502858	0.00846226	0.486229	0.519488
Drainage					
Affected	230	0.518246	0.0119674	0.494727	0.541764
Unaffected	230	0.487471	0.0119674	0.463953	0.510989
Regulation					
In oprarion	180	0.367058	0.0132043	0.341109	0.393007
Out of Opration	280	0.638658	0.010587	0.617853	0.659464
Drainage by Regulation					
Affected In oprario	90	0.412852	0.0186737	0.376155	0.449549
Affected Out of Opr	140	0.623639	0.0149723	0.594216	0.653063
Unaffected In oprario	90	0.321265	0.0186737	0.284568	0.357962
Unaffected Out of Opr	140	0.653677	0.0149723	0.624254	0.683101

The StatAdvisor
This table shows the mean NDVI for each level of the factors. It also shows the standard error of each mean, which is a measure of its sampling variability. The rightmost two columns show 95.0% confidence intervals for each of the means. You can display these means and intervals by selecting Means Plot from the list of Graphical Options.

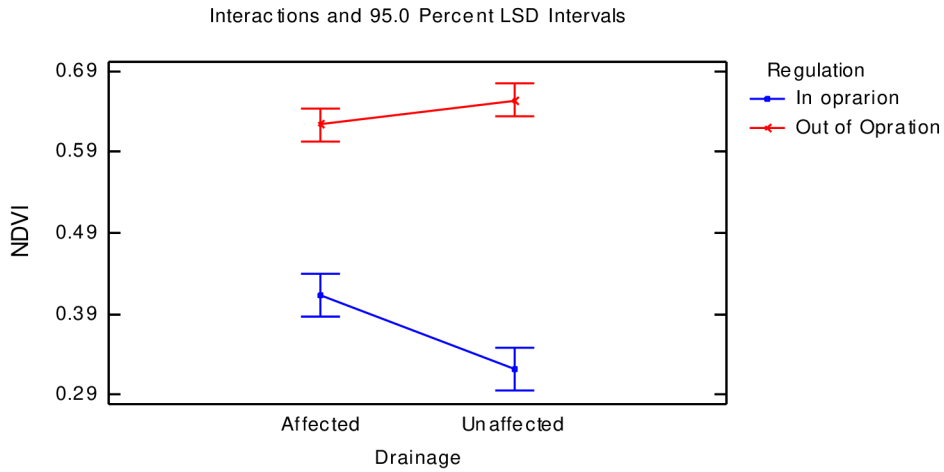

Multiple Comparisons for NDVI by Drainage

Method: 95.0 percent LSD

Drainage	*Count*	*LS Mean*	*LS Sigma*	*Homogeneous Groups*
Unaffected	230	0.487471	0.0119674	X
Affected	230	0.518246	0.0119674	X

Contrast	*Sig.*	*Difference*	*+/- Limits*
Affected - Unaffected		0.0307745	0.0332598

* denotes a statistically significant difference.

The StatAdvisor

This table applies a multiple comparison procedure to determine which means are significantly different from which others. The bottom half of the output shows the estimated difference between each pair of means. There are no statistically significant differences between any pair of means at the 95.0% confidence level. At the top of the page, one homogenous group is identified by a column of X's. Within each column, the levels containing X's form a group of means within which there are no statistically significant differences. The method currently being used to discriminate among the means is Fisher's least significant difference (LSD) procedure. With this method, there is a 5.0% risk of calling each pair of means significantly different when the actual difference equals 0.

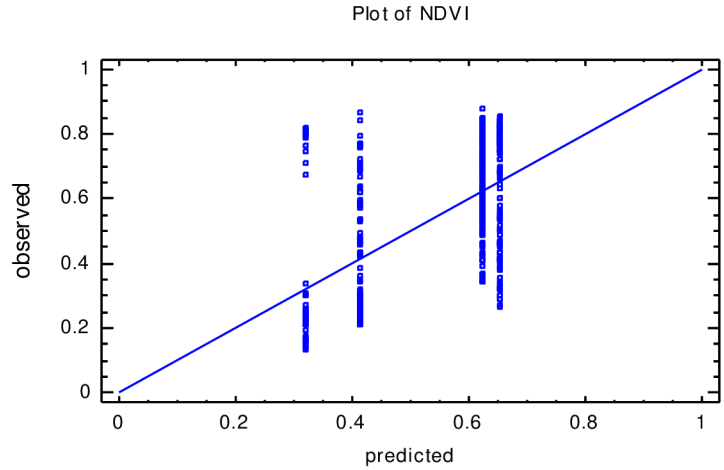

Regression Results for NDVI

	Fitted	*Stnd. Error*	*Lower 95.0% CL*	*Upper 95.0% CL*	*Lower 95.0% CL*	*Upper 95.0% CL*
Row	*Value*	*for Forecast*	*for Forecast*	*for Forecast*	*for Mean*	*for Mean*

The StatAdvisor

This table contains information about NDVI generated using the fitted model. The table includes:

(1) the predicted value of NDVI using the fitted model
(2) the standard error for each predicted value
(3) 95.0% prediction limits for new observations
(4) 95.0% confidence limits for the mean response

Each item corresponds to the values of the independent variables in a specific row of your data file. To generate forecasts for additional combinations of the variables, add additional rows to the bottom of your data file. In each new row, enter values for the independent variables but leave the cell for the dependent variable empty. When you return to this pane, forecasts will be added to the table for the new rows, but the model will be unaffected.

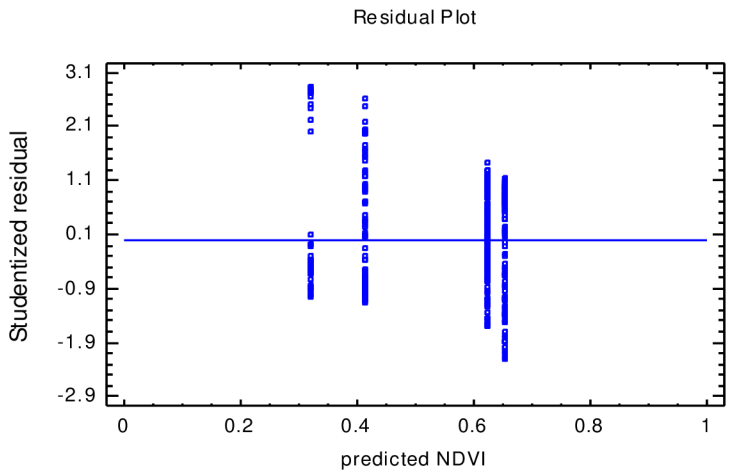

Unusual Residuals for NDVI

		Predicted		*Studentized*
Row	*Y*	*Y*	*Residual*	*Residual*
9	0.747889	0.321265	0.426624	2.43
31	0.803259	0.321265	0.481994	2.76
32	0.815454	0.321265	0.494189	2.83
38	0.290874	0.653677	-0.362804	-2.06
45	0.26953	0.653677	-0.384148	-2.19
46	0.301535	0.653677	-0.352142	-2.00
55	0.798757	0.321265	0.477492	2.73
77	0.804745	0.321265	0.48348	2.76
78	0.800535	0.321265	0.47927	2.74
101	0.817463	0.321265	0.496198	2.84
115	0.287801	0.653677	-0.365876	-2.08
123	0.801414	0.321265	0.480149	2.74
124	0.812284	0.321265	0.491019	2.81
137	0.265046	0.653677	-0.388632	-2.21
147	0.763522	0.321265	0.442257	2.53
169	0.803479	0.321265	0.482214	2.76
170	0.709707	0.321265	0.388442	2.21
193	0.788331	0.321265	0.467066	2.67
215	0.796032	0.321265	0.474767	2.71
216	0.672909	0.321265	0.351644	2.00
261	0.7693	0.412852	0.356448	2.03
285	0.844292	0.412852	0.431439	2.46
308	0.868861	0.412852	0.456009	2.60
331	0.795939	0.412852	0.383087	2.18
422	0.770518	0.412852	0.357666	2.04

The StatAdvisor

The table of unusual residuals lists all observations which have Studentized residuals greater than 2 in absolute value. Studentized residuals measure how many standard deviations each observed value of NDVI deviates from a model fitted using all of the data except that observation. In this case, there are 25 Studentized residuals greater than 2, but none greater than 3.

Influential Points for NDVI

		Mahalanobis		*Cook's*
Row	*Leverage*	*Distance*	*DFITS*	*Distance*
9	0.0111111	4.14825	0.258082	0.0164735
31	0.0111111	4.14825	0.292104	0.0210271
32	0.0111111	4.14825	0.299623	0.0221046
55	0.0111111	4.14825	0.289331	0.0206362
77	0.0111111	4.14825	0.29302	0.021157
78	0.0111111	4.14825	0.290426	0.0207901
101	0.0111111	4.14825	0.300862	0.0222847
123	0.0111111	4.14825	0.290968	0.0208665
124	0.0111111	4.14825	0.297668	0.021822
137	0.00714286	2.29714	-0.187533	0.00871785
147	0.0111111	4.14825	0.267669	0.017703
169	0.0111111	4.14825	0.29224	0.0210463
170	0.0111111	4.14825	0.234723	0.0136568
193	0.0111111	4.14825	0.282913	0.0197449
215	0.0111111	4.14825	0.287653	0.0204013
216	0.0111111	4.14825	0.212281	0.0111919
261	0.0111111	4.14825	0.215207	0.0114998
262	0.0111111	4.14825	0.207403	0.0106877
285	0.0111111	4.14825	0.261034	0.0168475
308	0.0111111	4.14825	0.276114	0.018821
331	0.0111111	4.14825	0.231453	0.0132829

354	0.0111111	4.14825	0.210322	0.0109881
422	0.0111111	4.14825	0.215949	0.0115785
423	0.0111111	4.14825	0.211404	0.0111005
445	0.0111111	4.14825	0.210377	0.0109937

Average leverage of single data point = 0.00869565

The StatAdvisor

The table of influential data points lists all observations which have leverage values greater than 3 times that of an average data point, or which have an unusually large value of DFITS or Cook's distance. Leverage is a statistic which measures how influential each observation is in determining the coefficients of the estimated model. DFITS is a statistic which measures how much the estimated coefficients would change if each observation was removed from the data set. Cook's distance measures the distance between the estimated coefficients with and without each observation. In this case, an average data point would have a leverage value equal to 0.00869565. There are no data points with more than 3 times the average leverage. There are 25 data points with unusually large values of DFITS. There are no data points with unusually large values of Cook's distance.